Structural Characterization of the Transmembrane-Juxtamembrane Region of Fibroblast Growth Factor Receptor 3

(繊維芽細胞増殖因子受容体 3 の
膜貫通-膜近傍部位の機能構造解析)

Hiroko Tamagaki
Graduate School of Science
Osaka University
2015

Contents

Abbreviations

A.A.	amino acid
Acm	actetamidomethyl
ATP	adenosine triphosphate
ATR	attenuated total reflection
Boc	*tert*-but768oxycarbonyl
Bzl	benzyl
C18	1,2-dioctadecanoyl-*sn*-glycero-3-phosphocholine
C19	1,2-dinonadecanoyl-*sn*-glycero-3-phosphocholine
CBD	chitin binding domain
CMC	critical micelle concentration
DARR	dipolar assisted rotational resonance
DCC	*N,N'*-dicyclohexylcarbodiimide
DCM	dichloromethane
DIEA	*N,N*-diisopropylethylamine
DMF	*N,N*-dimethylformamide
DMPC	1,2-dimyristoyl-*sn*-glycero-3-phosphocholine
DMPG	1,2-dimyristoyl-*sn*-glycero-3-[phosphor-rac-(1-glycerol)]
DTT	dithiothreitol
ECD	extracellular domain
E.coli	*Escherichia coli*
EDTA	ethylenediaminetetraacetic acid

EGF	epidermal growth factor
EGFR	epidermal growth factor receptor
EJM	extracellular juxtamembrane
ErbB	human epidermal growth factor receptor
ESI	electrospray ionization
FGF	fibroblast growth factor
FGFR	fibroblast growth factor receptor
Fmoc	9-fluorenylmethoxycarbonyl
FT-IR	fourier transform infrared spectroscopy
GpA	glycophorin A
Grb	growth factor receptor-bound protein
HBTU	2-(1H-benzotriazol-1-yl)-1,1,3,3-tetramethyluronium hexafluorophosphate
HEK293	human embryonic kidney 293 cells
HEPES	4-(2-hydroxyethyl)-1-piperazineethanesulfonic acid
HOBt	1-hydroxybenzotriazole
HOOBt	3,4-dihydro-3-hydroxy-4-oxo-1,2,3-benzotriazine
ICD	intracellular domain
IJM	intracellular juxtamembrane
IPTG	isopropyl β-D-1-thiogalactopyranoside
JAK-STAT	janus kinases-signal transducers and activators of transcription
JM	juxtamembrane
LB	lysogeny borth

LUV	large unilamellar vesicle
MALDI	matrix-assisted laser desorption/ionization
MAPK	ras-mitogen-activated protein kinase
MAS	magic angle spinning
MBHA resin	4-methylbenzhydrylamine hydrochloride salt resin
MES	2-(*N*-morpholino)ethanesulfonic acid
MESNA	sodium 2-mercaptoethanesulfonate
Mex gyrA	*Mycrobasterium xenopi gyrase A*
MOPS	3-morpholinopropane-1-sulfonic acid
Ni-NTA	nickel nitrilotriacetic acid
NMP	1-methyl-2-pyrrolidinone
NMR	nuclear magnetic resonance
OG	*n*-octyl-β-glucoside
PCR	polymerase chain reaction
Pbf	2,2,4,6,7-pehtamethyl-2,3-dihydrobenzofuran-5-sulfonyl
PEG	polyethylene glycol
PIP_2	phosphatidyliositol 4,5-bisphodphate
PLC-γ	phospholipase Cγ
POPC	1-palmitoyl-2-oleoyl-*sn*-glycero-3-phosphocholine
POPS	1-palmitoyl-2-oleoyl-*sn*-glycero-3-phospho-L-serine
PS	phospho-L-serine
RP-HPLC	reversed-phase high performance liquid chromatography

RTK	receptor tyrosine kinase
SAL resin	super acid-labile resin (Rink amide resin)
SDS-PAGE	sodium dodecylsulfate polyacrylamide gel electrophoresis
*t*Bu	tertiary butyl
TCEP	tris(2-carboxyethyl)phosphine
TFA	trifluoroacetic acid
Thz	thiazolidine
TM	transmembrane
TOF	time-of-flight
Tos	tosyl
Tris	2-amino-2-hydroxymethyl-propane-1,3-diol
Trt	trityl
Z	benzyloxycarbonyl

Abstract

Fibroblast growth factor receptors (FGFRs) constitute one of the subfamilies in receptor tyrosine kinase (RTKs). Four FGFRs, namely, FGFR1, FGFR2, FGFR3 and FGFR4, are known to mediate a variety of cellular responses during embryonic development. Dysregulation of FGFR signaling is associated with many developmental disorders and cancer[1]. The prototypical FGFR comprised of an excellular region, a single transmembrane (TM) region, and a cytoplasmic region. The crystal structures of the extracellular[2,3] and the intracellular[4-6] regions of FGFR3 have provided considerable information in elucidating the mechanism underlying receptor signaling. However, there is still no high-resolution of a full-length RTK. The mechanism emerging from structural and biochemical involve binding of the fibroblast growth factor (FGF) to the extracellular domain (ECD) of the receptor in a 1: 1 complex. These complexes are thought to form a symmetric dimer in the active state[7]. High-resolution structures of activated kinase domain for FGFR1[4], FGFR2[5] and FGFR3[6] demonstrated that they form asymmetric dimers. Importantly, Bae et al. demonstrated that formation of asymmetric dimers between the FGFR1 kinase domains is required for transphosphorylation in FGF-stimulated cell[4].

The proposed activation mechanism of FGFR based on the crystal structure, builds on that proposed by Kuriyan and coworkers for the EGF receptor[8]. An open question has been how a symmetric extracellular domain dimer leads to asymmetric interactions in the interacellular domains. In the case of EGF receptor family, the coupling of ligand binding is to receptor activation is of great interest since the interacellular

juxtamembrane (IJM) region is allosterically coupled to the ligand-binding site[9,10]. Recently, we examined the functional coupling of the extracellular and intracellular regions by the TM and the IJM regions of the rat ErbB2/Neu receptor via the TM and the IJM regions[11], by comparing the structure of the TM-IJM sequences of the wild type and a constitutively active TM region in a mutant (V664E). Solid-state NMR and fluorescence spectroscopy of these peptides, reconstituted into lipid bilayer, demonstrated that the TM helices of the V664E mutant dimerized more tightly than in the wild type construct. In addition, the unstructured IJM region of the wild type sequence was bound to the acidic membrane, while the mutant IJM region was not bound to the membrane; IJM release was dependent on the orientation of the TM helices in the membrane. We concluded that the TM helices in the active dimer conformation could release the IJM region from the membrane, triggering the formation of an asymmetric dimer between the intracellular kinase regions. Endres et al. proposed a similar model based on the detailed biochemical and structural analyses of the EGFR[8].

This thesis describes the structural characterization of the FGFR3 TM-IJM region in order to elucidate its role in activation. In the first section (**Chapter 1**); the preparation of TM-IJM sequence of FGFR3 by means of chemical synthesis is described. Chemical synthesis allows specific labeling and modification, extending the choice of analytical techniques.

The second section (**Chapter 2 and 3**) focuses on the structural characterization of the TM-IJM region of FGFR. Spectroscopic structural comparison between the wild type and the constitutively active mutant were performed to determine the IJM-membrane

interaction, TM helix orientation relative to the membrane, and the TM helices dimer interface. Finally, the results of the structural comparison are summarized, and an activation mechanism of FGFR3 is discussed.

Furthermore, the challenges involved in the semi-synthesis of FGFR3 are addressed to understand the structural change of TM-JM region upon ligand binding (**Chapter 4**). Semi-synthesis can be carried out by ligating expressed protein fragments and chemically synthesized peptides, which can contain specific labels and modifications. The initial results mentioned in this thesis provide a basis for a novel research strategy using semi-synthetic membrane proteins.

Introduction

There are various receptors in the plasma membrane, which play pivotal roles in signal transduction. Detection of a specific membrane-binding site for the epidermal growth factor (EGF) and subsequent discovery of its receptor (EGFR) by Cohen and Carpenter[12,13], have led to the recognition that receptor tyrosine kinases (RTK) hold great importance in cell homeostasis. Human cells contain 58 RTKs involved in cell growth and differentiation. RTKs are commonly comprised of three distinct regions: the extracellular, transmembrane, and intracellular domains. The extracellular domain (ECD) contains the ligand-binding site, and the intracellular domain (ICD) possesses the kinase activity. The transmembrane (TM) region functionally couples to the soluble regions.

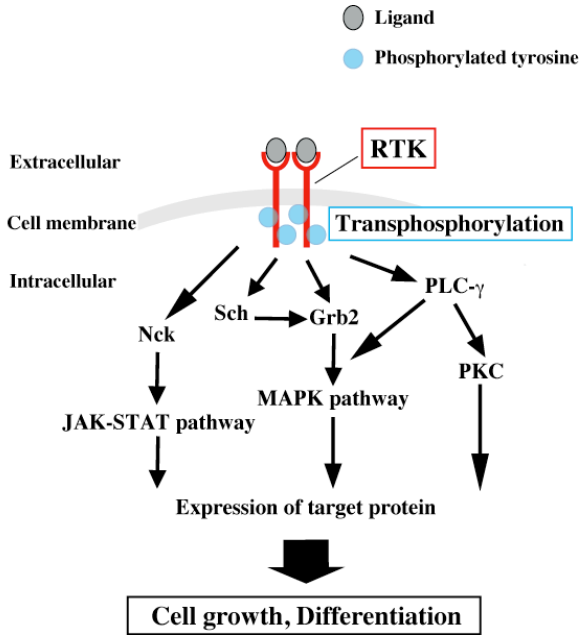

Figure 1. Schematic diagram of RTK signal transduction. Activated RTK induces various signal transduction cascades.

Figure 1, illustrates a schematic diagram of RTK signaling. A ligand such as growth factor binds to the ECD of the RTK and induce transphosphorylation in the ICD. The phosphorylated RTK activates the adaptor proteins and phospholipase Cγ (PLC-γ) stimulating pathways such as the Ras-mitogen-activated protein kinase (MAPK) pathway, and the Janus kinases-signal transducers and activators of transcription (JAK-STAT) pathway. Finally, the target protein is expressed, inducung the cell growth and differentiation[14].

RTK dysfunction, as a result of mutation or overexpression, is known to be related to a number of diseases such as cancer, cardiovascular, inflammatory and nervous disorders. Natutrally, RTK has become one of the most important targets for cancer therapy. In 1985, Drebin et al. found that a monoclonal antibody can induce a rapid and reversible down-regulation of cell surface expressed oncogenic RTK (ErbB2/Neu)[15]. This finding advanced the development of cancer therapeutics targeting to the ECD. For targeting the ICD, small compounds drugs have been developed as kinase inhibitors. The inhibitors are designed to act on the ATP binding pocket within the kinase region[16]. Despite the existence of a number of therapeutic products, a demand for better cancer treatment drugs remains. A stronger understanding of the function of RTK at the membrane, particularly at a molecular level or at higher resolution, can provide insight for the design of new drugs.

The initial model of the RTK activation is described as ligand-binding stabilized dimerization. In 1988, Schlessinger described the activation mechanism of EGFR as the allosteric receptor oligomerization model[17]. It is assumed that monomeric inactive

receptors are in equilibrium with oligomeric activated receptors. According to the allosteric oligomerization model, the binding of growth factor(s) to their receptor(s) stabilizes an oligomeric state possessing enhanced ligand-binding affinity and elevated protein tyrosine kinase activity. The model has been considered as a "textbook" description for RTK activation since.

Recent studies elucidating the activation mechanism suggest that the actual mechanism is more complicated than the initial model. One important finding is that dimerization is not sufficient for activation. A number of studies suggest that EGFRs also exist as inactive dimers at the membrane[18-20]. These reports argue that there must be an inhibitory effect for the preformed dimer and this effect is overcome by ligand-binding induced structural change within the dimer.

Although a full-length structure has yet to be reported, a number of crystal structures of the ECD and the ICD of several RTKs have been elucidated. The crystal structures of the EGFR ECD, in both ligand bound and unbound forms[21,22], have suggested that the unliganded structure has a tethered conformation that undergoes a dramatic rearrangement upon binding to the ligand. Significant crystallographic and biochemical findings reported by Kuriyan et al. have demonstrated that ICDs form active asymmetric dimers[23] and that the intracellular juxtamembrane (IJM) region participates in the dimerization of the kinase domains[24]. These important discoveries regarding both the ECD and ICD raise a fundamental question concerning transmembrane receptors: how is a structural change in an extracellular region transmitted to the intracellular region, which then results in activity. This also emphasizes the requirement

for a structure-function study of the TM region.

A study of the oncogenic protein p185, which is now known as ErbB2 or Neu, is the earliest to suggest an active role of the TM region in receptor function[25]. A V664E mutation in the TM region (rat sequence) is sufficient for activation of the Neu receptor. Subsequent studies by Smith et al. demonstrated that in the active receptor containing the V664E point mutation, Glu664 mediates dimerization through hydrogen-bond interactions[26]. Stern et al. has also reported that changing the relative position of $VE_{664}G$ sequence within the TM region promotes weak dimerization but not transformation[27]. These findings suggest that the dimerization of the TM region is not sufficient for receptor function. The IJM region was also found to play an active role in EGFR function. The juxtamembrane is defined in this study as the region adjacent to the TM region, approximately 15 amino acid residues in length. This definition differs from the one used by Kuriyan et al. mentioned previously. As shown in **Figure 2**, the IJM region of EGFR is highly basic; this basic cluster can be found in a number of RTKs (**Figure 2**). One of the earliest studies of this minute region revealed that phosphorylation of a threonine residue (Thr654) down-regulated EGFR[28,29]. Additionally, Yamane et al. reported that ligand-induced functions of EGFR require positively charged residues in this IJM region[30]. In 2005, McLaughlin et al. proposed a model suggesting that the IJM region is crucial for understanding the EGFR activation mechanism[31]. The model describes the autoinhibitory mechanism of EGFR; in the inactive receptor, the IJM and kinase domains associate electrostatically with the negatively charged plasma membrane, restricting access of the kinase domain to its

substrate. An important feature of the IJM region is that this positively charged region binds to the membrane sequestering phosphatidylinositol 4,5-bisphosphate (PIP_2), known to be involved in the EGFR signaling cascade as the source of a secondary messenger. Furthermore, Sato et al. reported that this interaction between the IJM region and the acidic membrane is diminished with the addition of Ca^{2+}/calmodulin[32]. Ca^{2+}/calmodulin is known to bind to the IJM region and mediates EGFR signaling[33-35]. In addition, Ca^{2+}/calmodulin interacts with the IJM region removing it from the membrane, thus increasing the separation time of the kinase domain from the membrane[36]

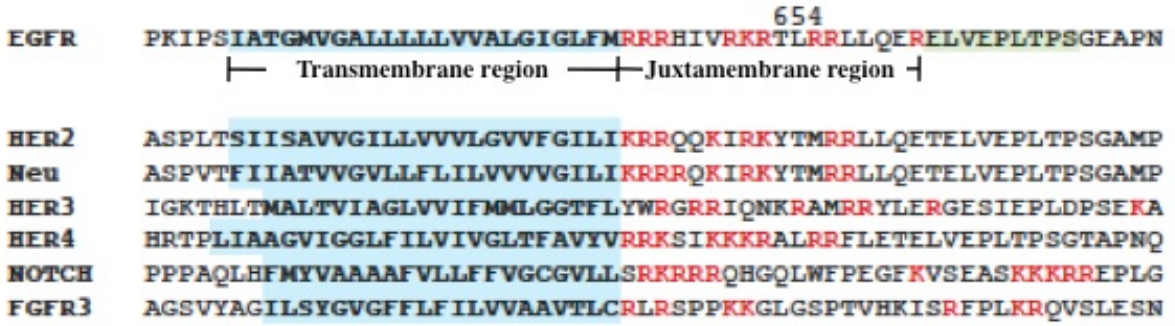

Figure 2. Sequence of the RTK transmembrane-intracellular juxtamembrane (TM-IJM) region. The TM region is highlighted in blue. The juxtamembrane (IJM) region, defined in this study, follows immediately after the TM region. The EGFR juxtamembrane region defined by Kuriyan et al. is highlighted in green.

Sato and coworkers extended McLaughlin's studies by examining how release of the IJM from the membrane is related to the TM helices dimer structure. Peptides of the ErbB2/Neu receptor TM-IJM sequence were chemically synthesized with or without activating mutation V664E in the TM region, and structural studies were performed. They found that introduction of the constitutively active mutation facilitates the release

of the IJM region from the membrane, and proposed an activation mechanism for ErbB that is illustrated in **Figure 3**[11]. Interestingly, Kuriyan's group reported a similar model based on their biochemical and structural studies on EGFR TM-IJM region. The model is also supported by molecular dynamics simulation research performed by Shaw's group[37]. An important feature of the model is that the release of the IJM region triggers the formation of the active dimer in the ICD.

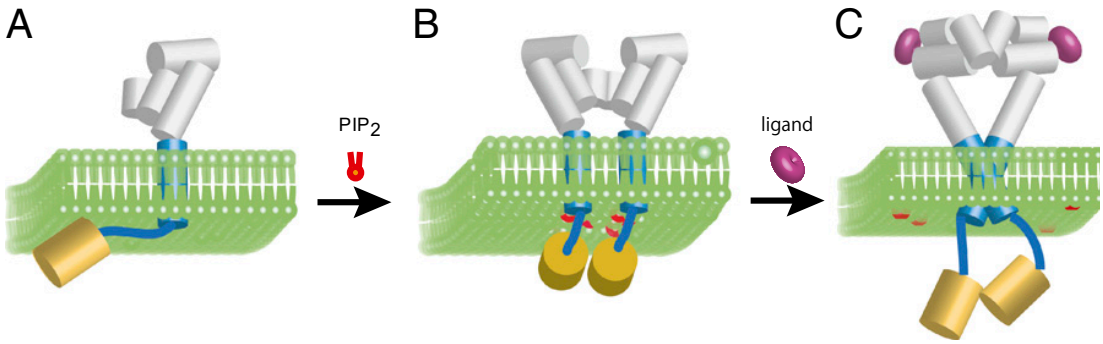

Figure 3. The activation mechanism of ErbB2/Neu, as suggested by Sato and coworkers. In the inactive state, the receptor IJM is bound to the membrane surface (A and B). Binding of the ligand to the ECD induces dimerization of the receptor and release of the IJM from the membrane surface resulting in activity (C).

Fibroblast growth factor receptor (FGFR) is an RTK known to be involved in cell growth and differentiation. FGFR was first isolated and cloned by Lee et al.[38], and additional members were discovered by homology based PCR[39-43]. Human cells are thought to contain four members of the FGFR family.

FGFRs share common structural features with other RTKs; they are comprised of three domains: the extracellular domain (ECD), transmembrane domain (TM), and the intracellular domain (ICD). Binding of the ligand to the ECD initiates signaling

cascades. Human cells have 18 FGFR ligands, and require a heparan sulfate proteoglycan for activity[44].

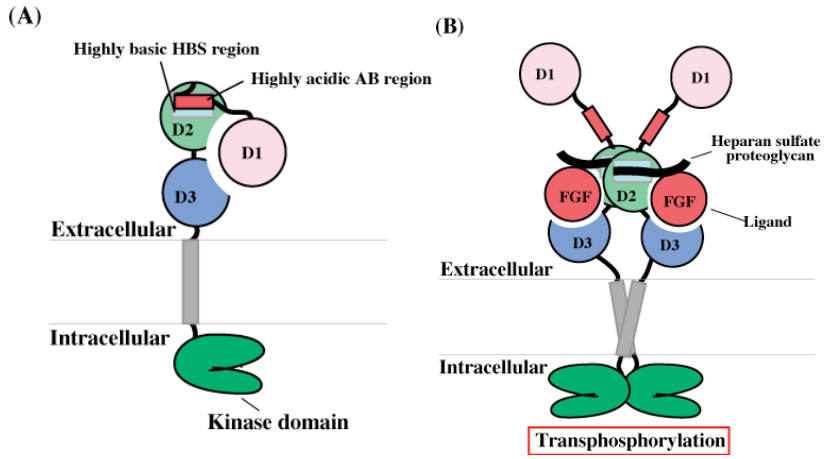

Figure 4. Schematic model of the FGFR extracellular domain (ECD)[7]. (A) The ECD of FGFR consists of three immunoglobulin domains D1, D2, and D3. In the inactive state, the highly acidic AB region of the D1-D2 linker binds to the highly basic HBS region of D2. D1 binds to D2 and D3 resulting in autoinhibition. (B) The FGF ligand binds to D2, D3 and the D2-D3 linker via hydrogen bonds. Heparan sulfate proteoglycan binds to the highly basic HBS region of D2. These bonds in the ECD induce dimer formation leading to the transphosphorylation of the intracellular region kinase domain for activity.

The ECD consists of three immunoglobulin-like subdomains called D1, D2 and D3. D2 and D3 are suggested to constitute the minimal ligand binding region[2,45,46]. Mohammadi and coworkers reported the crystal structure of FGFR3 ECD and FGF1[46], and proposed a model for autoinhibiton of FGFR that involves D1 suppression of FGF and heparin binding[7,46]. Prior to ligand and heparin binding in the ECD (i.e. inactive state), D1 binds to D2 and D3, and the D1-D2 linker region, which contains a highly acidic sequence called the acid box (AB), binds to the highly basic region in D2 resulting in autoinhibition (**Figure 4 (A)**). The Ligand and heparin form hydrogen

bonds with specific sites in D2 and D3 creating a symmetric dimer of FGFR: FGF (2:2) together with heparin (**Figure 4 (B)**). Dimer formation resulting from ligand binding in the ECD induces the transphosphorylation of the ICD for activity.

Binding of the ligand in the ECD is suggested to induce dimer formation and transphosphorylation in the ICD. Transphosphorylation in the catalytic domain of the ICD that stimulates the kinase activity[47,48]. The phosphorylated tyrosine at the C-terminal tail of the ICD is involved in initiating the cascade as summarized in Figure 1. The activated FGFR3 kinase domains are proposed to form an asymmetric dimer[4-6]. The asymmetric dimer is formed by the substrate-acting kinase and the enzyme-acting kinase (**Figure 5**).

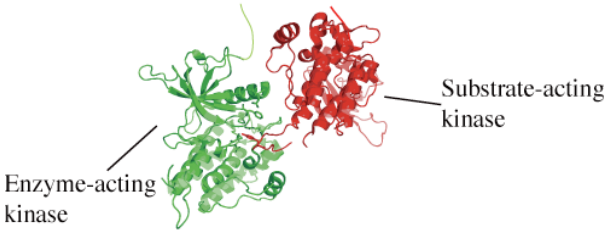

Figure 5. Model of the asymmetric ICD dimer (based on PDB code 4K33). The asymmetric dimer is comprised of the enzyme-acting kinase and the substrate-acting kinase leading to transphosphorylation.

The structure and functional relationship of the TM region are not well known. However, a number of pathogenic FGFR mutations in the TM and juxtamembrane (JM) regions have been identified (reviewed in reference[49]), suggesting that these regions play an active role in receptor function.

Hristova's group has been studied the biophysical properties of the FGFR3 TM region by comparing sequences with and without activating mutations[49-55]. Two mutations in

the TM region of FGFR3, G380R and A391E, are known to activate the receptor without ligand binding. The A391E mutation appears to be similar to the V664E mutation in the Neu receptor (i.e. substitution of a hydrophobic residue with glutamic acid). A391E is the genetic cause of Crozon syndrome[56], and has been additionally identified as a somatic mutation in bladder cancer[57]. This mutation can enhance FGFR3 activation in the absence of the ligand, and results in an increase in the dimerization propensity of the TM sequence alone in lipid bilayers[50], and of the full-length receptor at the cell membrane[55]. The G380R, which is related to achondroplasia[58], is the most common form of dwarfism. Hristova and coworkers reported that the TM region containing the G380R did not alter the dimerization energetic of the TM helices in lipid bilayers[51]. Recently, they demonstrated that the G380R mutation had only a modest effect on receptor dimerization in plasma membrane-derived vesicles from HEK293T cells. Kinase activity due to the G380R mutation could be attributed to a mutation-induced structural change rather than an increase in dimerization propensity[59]. It can be assumed that the TM region in each of these mutations is in the active dimer conformation.

However, the detailed structure of the TM region together with the JM region in lipid bilayers, and the structural changes undergone by the TM-JM region to induce activity are not known. In addition, the mechanism by which structural changes in the ECD caused by ligand binding are transmitted through the TM region to initiate the function of the ICD is also unknown (**Figure 6**).

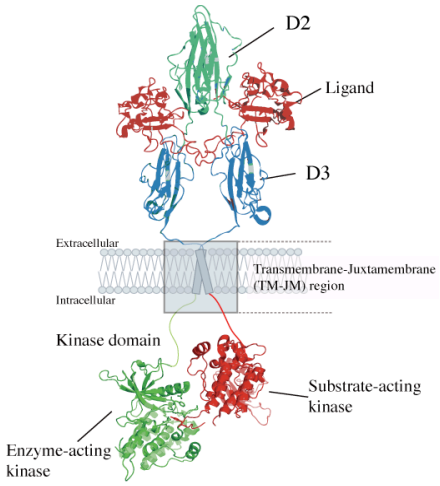

Figure 6. FGFR model: structural and biological information regarding the TM-JM region linking the ECD (from PDB code 1RY7) and ICD (from PDB code 4K33) is lacking. This information is required to understand the activation mechanism of FGFRs.

In this thesis, the author focuses the structure of TM-JM region to get insight on the activation mechanism of FGFR3. The structural information of TM-JM region in lipid bilayers is obtained from the spectroscopic experiments on chemically synthesized TM-JM peptide.

Peptide chemistry has been utilized to great effect in a wide range of scientific fields. It can be used as a tool to elucidate biological mechanisms or for the development of drugs and materials. One of the biggest advantages of chemical synthesis is that it allows for considerable variation in designing sequences, modifications and labels. The structural formation of membrane proteins and their association with the transmembrane (TM) region has been studied using chemically synthesized peptides. In studies such as those performed by Killian (for review[60]) or Matsuzaki (as one of their works[61]), an artificial TM peptide was designed to examine theories regarding TM sequences existing in the membrane. One of the earliest TM sequences to be

chemically synthesized was a section of glycophorin A (GpA)[62]. GpA is one of the first membrane proteins for which a sequence was reported[63]. Chemical synthesis of GpA enabled the study of TM helix association, which resulted in high-resolution structural information. Smith et al. used solid-state NMR to study the GpA TM peptide with site-specific stable isotope labels. Their results revealed that the dimer structure is mediated by a GxxxG sequence[64]. The GxxxG motif is now known to promote TM helix association in many membrane proteins.

Along with a long history of peptide chemistry, the introduction of a solid phase method for peptide synthesis, invented by Merrifield[65], increased the use of peptides in a variety of fields. The solid phase method usually involves the elongation of a side chain protected peptide chain on a polystyrene resin. Subsequent to elongation, the peptide chain is cleaved from the resin by acid treatment. Coupled with reverse phase high-performance liquid chromatography (RP-HPLC) purification, a 30-50 amino acid length peptide can be obtained. This method, which allows for rapid and simple peptide preparation, is intrinsically limited in the length of peptide that can be synthesized. Ligation chemistry, as a strategy for chemical synthesis of proteins or longer peptides, was introduced by Hojo and Aimono[66]. As shown in **Figure 7 (A)**, a peptide with a thioester moiety at the C-terminus is required as a building block. The thioester moiety is crucial for ligation chemistry since it enables selective activation of the C-terminus of the N-terminal building blocks. In this strategy, designated as the thioester method, selective activation is performed by a silver ion. The silver ion activated thioester moiety is exchanged with an additive, 3,4-dihydro-3-hydroxy-4-oxo-1,2,3-benzotriazine

(HOOBt), which subsequently enables peptide bond formation for condensation. Another ligation strategy, native chemical ligation, was proposed by Kent et al. as shown in **Figure 7 (B)**[67]. Native chemical ligation also requires a peptide thioester as the N-terminal building block. The thioester moiety in the N-terminal building block interacts with the cysteine residue at the N-terminus of the C-terminal building block. The reaction is initiated by a thioester-thiol exchange followed by spontaneous rearrangement to form a peptide bond.

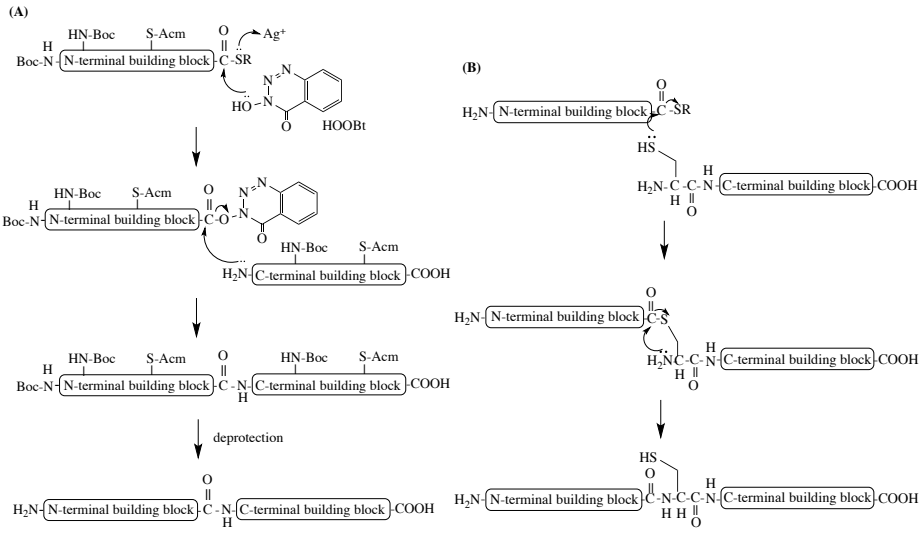

Figure 7. Schemes of the thioester method **(A)** and native chemical ligation **(B)**.

As previously mentioned, ligation involves a key thioester. Protein fragments containing a thioester moiety at their C-terminus can be obtained using molecular biology techniques and intein chemistry. Protein splicing, discovered separately by Anraku et al.[68] and Stevens[69], is a post-translational process in which an intervening portion of a precursor protein is excised and the flanking N-terminal and C-terminal sequences are coupled to give a mature protein. As defined by Perler et al.[70], the intervening portion and the flanking sequences are called intein and extein, respectively.

As illustrated in **Figure 8 (A)**, protein splicing is initiated by an N-to-S acyl shift and the N-extein sequence is transferred to the –SH/-OH side chain of a Cys/Ser located at the N-terminus of the intein portion. This newly formed ester is attacked by the side chain of a Cys/Ser/Thr located at the N-terminus of the C-extein sequence to give the mature protein. Muir et al. developed a novel strategy for preparing a protein fragment containing a thioester moiety at its C-terminus[71,72]. As shown in **Figure 8 (B)**, instead of the C-extein, they inserted a chitin beads sequence. Subsequent to washing, the desired protein fragment containing the thioester moiety at the C-terminus is eluted by addition of excess thiol. This strategy allows for the preparation of large protein building blocks for ligation, which is known as expressed protein ligation.

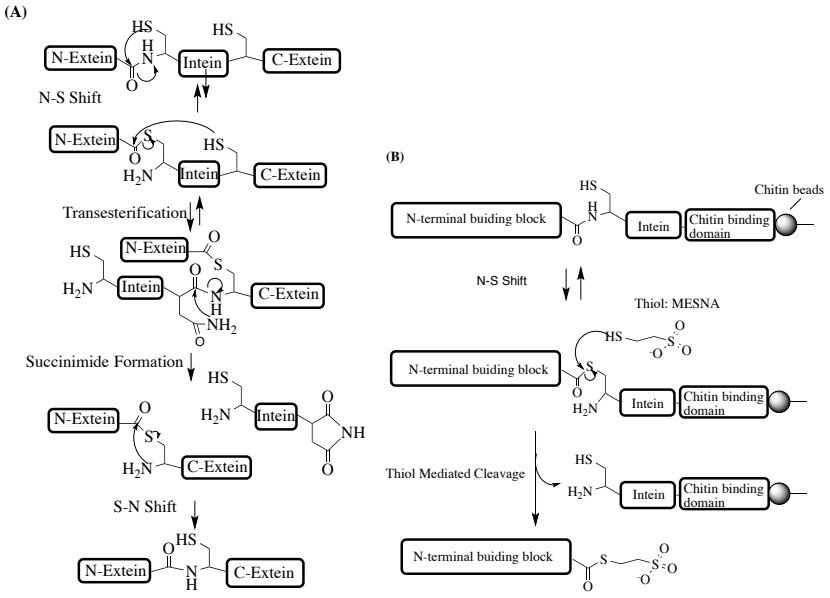

Figure 8. Schemes of intein chemistry (A) and (B)preparation of N-terminal building blocks containing a thioester at the C-terminus using intein chemistry.

1. Eswarakumar, V.P., Lax, I. & Schlessinger, J. Cellular signaling by fibroblast growth factor receptors. *Cytokine Growth Factor Rev*. **16**, 139-149 (2005).
2. Plotnikov, A.N., Schlessinger, J., Hubbard, S.R. & Mohammadi, M. Structural basis for FGF receptor dimerization and activation. *Cell* **98**, 641-650 (1999).
3. Plotnikov, A.N., Hubbard, S.R., Schlessinger, J. & Mohammadi, M. Crystal structures of two FGF-FGFR complexes reveal the determinants of ligand-receptor specificity. *Cell* **101**, 413-424 (2000).
4. Bae, J.H., Boggon, T. J., Tomé, F., Madfiyan V., Lax I. & Schlessinger J. Asymmetric receptor contact is required for tyrosine autophosphorylation of fibroblast growth factor receptor in living cells. *Proc. Natl. Acad. Sci. U. S. A.* **107**, 2866-2871 (2010).
5. Chen, H., Xu, C. F., Ma, J., Eliseenkova, A. V., Li W., Pollock P. M., Pitteloud N., Miller W.T., Neubert, T. A. & Mohammadi, M. A. crystallographic snapshot of tyrosine trans-phosphorylation in action. *Proc. Natl. Acad. Sci. U. S. A.* **105**, 19660-19665 (2008).
6. Huang, Z., Chen, H., Blais S., Neubert, T. A., Li X. & Mohhamadi, M. Structural mimicry of a-loop tyrosine phosphorylation by a pathogenic FGF receptor 3 mutation. *Structure* **21**, 1889-96 (2013).
7. Mohammadi, M., Olsen, S.K. & Ibrahimi, O.A. Structural basis for fibroblast growth factor receptor activation. *Cytokine Growth Factor Rev*. **16**, 107-137 (2005).
8. Endres, N.F., Das, R., Smith, A. W., Arkhipov, A., Kovacs, E., Huang, Y., Pelton, J. G., Shan, Y., Shaw, D. E., Wemmer, D. E., Groves, J. T. & Kuriyan, J. Conformational Coupling across the Plasma Membrane in Activation of the EGF Receptor. *Cell* **152**, 543-556 (2013).
9. Macdonald-Obermann, J.L. & Pike, L.J. The intracellular juxtamembrane domain of the epidermal growth factor (EGF) receptor is responsible for the allosteric regulation of EGF binding. *J. Biol. Chem*. **284**, 13570-6 (2009).
10. Macdonald-Obermann, J.L. & Pike, L.J. Palmitoylation of the EGF receptor impairs signal transduction and abolishes high-affinity ligand binding. *Biochemistry* **48**, 2505-13 (2009).
11. Matsushita, C., Tamagaki, H., Miyazawa, Y., Aimoto, S., Smith, S. O. & Sato, T. Transmembrane helix orientation influences membrane binding of the intracellular juxtamembrane domain in Neu receptor peptides. *Proc. Natl. Acad. Sci. U. S. A.* **110**, 1646-1651 (2013).

12. Carpenter, G., Lembach, K.J., Morrison, M.M. & Cohen, S. Characterization of Binding of I-125-Labeled Epidermal Growth-Factor to Human Fibroblasts. *J. Biol. Chem.* **250**, 4297-4304 (1975).

13. Carpenter, G., King, L. & Cohen, S. Epidermal Growth-Factor Stimulates Phosphorylation in Membrane Preparations Invitro. *Nature* **276**, 409-410 (1978).

14. Marmor, M.D., Skaria, K.B. & Yarden, Y. Signal transduction and oncogenesis by ErbB/HER receptors. *Int. J. Radiat. Oncol. Biol. Phys.* **58**, 903-13 (2004).

15. Drebin, J.A., Link, V.C., Stern, D.F., Weinberg, R.A. & Greene, M.I. Down-modulation of an oncogene protein product and reversion of the transformed phenotype by monoclonal antibodies. *Cell* **41**, 697-706 (1985).

16. Zhang, H., Berezov, A., Wang, Q., Zhang, G., Drebin, J., Murai, R. & Greene, M. I. ErbB receptors: from oncogenes to targeted cancer therapies. *J. Clin. Invest.* **117**, 2051-8 (2007).

17. Schlessinger, J. Signal transduction by allosteric receptor oligomerization. *Trends Biochem. Sci.* **13**, 443-7 (1988).

18. Chung, I., Akita, R., Vandlen, R., Toomre, D., Schlessinger, J. & Mellman I. Spatial control of EGF receptor activation by reversible dimerization on living cells. *Nature* **464**, 783-U163 (2010).

19. Moriki, T., Maruyama, H. & Maruyama, I.N. Activation of preformed EGF receptor dimers by ligand-induced rotation of the transmembrane domain. *J. Mol. Biol.* **311**, 1011-1026 (2001).

20. Sako, Y., Minoghchi, S. & Yanagida, T. Single-molecule imaging of EGFR signalling on the surface of living cells. *Nat. Cell Biol.* **2**, 168-72 (2000).

21. Ogiso, H., Ishitani, R., Nureki, O., Fukai, S., Yamanaka, M., Kim, J. H., Saito, K., Sakamoto, A., Inoue, M., Shirouzu, M. & Yokoyama, S. Crystal structure of the complex of human epidermal growth factor and receptor extracellular domains. *Cell* **110**, 775-787 (2002).

22. Ferguson, K.M., Berger M. B., Mendrola J.M., Cho H. S., Leahy D. J. & Lemmon M.A. EGF activates its receptor by removing interactions that autoinhibit ectodomain dimerization. *Mol. Cell* **11**, 507-517 (2003).

23. Zhang, X.W., Gureasko, J., Shen, K., Cole, P.A. & Kuriyan, J. An allosteric mechanism for activation of the kinase domain of epidermal growth factor receptor. *Cell* **125**, 1137-1149 (2006).

24. Jura, N., Endres, N. F., Engel, K., Deindl, S., Das, R., Lamers, M. H., Wemmer D. E., Zhang, X. & Kuriyan, J. Mechanism for Activation of the EGF Receptor Catalytic Domain by the Juxtamembrane Segment. *Cell* **137**, 1293-1307 (2009).

25. Bargmann, C.I., Hung, M.C. & Weinberg, R.A. Multiple Independent Activations of the Neu Oncogene by a Point Mutation Altering the Transmembrane Domain of P185. *Cell* **45**, 649-657 (1986).

26. Smith, S.O., Smith, C.S. & Bormann, B.J. Strong hydrogen bonding interactions involving a buried glutamic acid in the transmembrane sequence of the neu/erbB-2 receptor. *Nat. Struct. Biol.* **3**, 252-258 (1996).

27. Burke, C.L., Lemmon, M.A., Coren, B.A., Engelman, D.M. & Stern, D.F. Dimerization of the p185(neu) transmembrane domain is necessary but not sufficient for transformation. *Oncogene* **14**, 687-696 (1997).

28. Hunter, T. & Cooper, J.A. Epidermal Growth-Factor Induces Rapid Tyrosine Phosphorylation of Proteins in A431 Human-Tumor Cells. *Cell* **24**, 741-752 (1981).

29. Hunter, T., Ling, N. & Cooper, J.A. Protein kinase C phosphorylation of the EGF receptor at a threonine residue close to the cytoplasmic face of the plasma membrane. *Nature* **311**, 480-3 (1984).

30. Yamane, K., Toyoshima, C. & Nishimura, S. Ligand-Induced Functions of the Epidermal Growth-Factor Receptor Require the Positively Charged Region Asymmetrically Distributed across Plasma-Membrane. *Biochem. Biophys. Res. Commun.* **184**, 1301-1310 (1992).

31. McLaughlin, S., Smith, S.O., Hayman, M.J. & Murray, D. An electrostatic engine model for autoinhibition and activation of the epidermal growth factor receptor (EGFR/ErbB) family. *J. Gen. Physiol.* **126**, 41-53 (2005).

32. Sato, T., Pallavi, P., Golebiewska, U., McLaughlin, S. & Smith, S.O. Structure of the membrane reconstituted transmembrane-juxtamembrane peptide EGFR(622-660) and its interaction with Ca2+/calmodulin. *Biochemistry* **45**, 12704-12714 (2006).

33. Martin-Nieto, J. & Villalobo, A. The human epidermal growth factor receptor contains a juxtamembrane calmodulin-binding site. *Biochemistry* **37**, 227-236 (1998).

34. Li, H.B., Ruano, M.J. & Villalobo, A. Endogenous calmodulin interacts with the epidermal growth factor receptor in living cells. *FEBS Lett.* **559**, 175-180 (2004).

35. Sanchez-Gonzalez, P., Jellali, K. & Villalobo, A. Calmodulin-mediated regulation of the epidermal growth factor receptor. *FEBS J.* **277**, 327-342 (2010).

36. Sengupta, P., Bosis, E., Nachliel, E., Gutman, M., Smith, S. O., Mihályné, G., Zaitseva, I. & McLaughlin, S. EGFR Juxtamembrane Domain, Membranes, and Calmodulin: Kinetics of Their Interaction. *Biophy. J.* **96**, 4887-4895 (2009).

37. Arkhipov, A., Chan, Y., Das, R., Endres, N. F., Eastwood, M. P., Wemmer, D. E., Kuriyan, J. & Shaw, D. E. Architecture and Membrane Interactions of the EGF Receptor. *Cell* **152**, 557-569 (2013).

38. Lee, P.L., Johnson, D.E., Cousens, L.S., Fried, V.A. & Williams, L.T. Purification and complementary DNA cloning of a receptor for basic fibroblast growth factor. *Science* **245**, 57-60 (1989).

39. Isacchi, A., Bergonzoni, L. & Sarmientos, P. Complete sequence of a human receptor for acidic and basic fibroblast growth factors. *Nucleic Acids Res.* **18**, 1906 (1990).

40. Pasquale, E.B. A distinctive family of embryonic protein-tyrosine kinase receptors. *Proc. Natl. Acad. Sci. U. S. A.* **87**, 5812-6 (1990).

41. Dionne, C.A., Crumley, G., Bellot, F., Kaplow, J. M., Searfoss, G., Ruta, M., Burgess, W. H., Jaye, M. & Schlessinger, J. Cloning and expression of two distinct high-affinity receptors cross-reacting with acidic and basic fibroblast growth factors. *EMBO J.* **9**, 2685-92 (1990).

42. Horlick, R.A., Stack, S.L. & Cooke, G.M. Cloning, expression and tissue distribution of the gene encoding rat fibroblast growth factor receptor subtype 4. *Gene* **120**, 291-5 (1992).

43. Partanen, J., Mäkelä, T. P., Eerola, E., Korhonen, J., Hirvonen, H., Claesson-Welsh, L. & Alitalo, K. FGFR-4, a novel acidic fibroblast growth factor receptor with a distinct expression pattern. *EMBO J.* **10**, 1347-54 (1991).

44. Yayon, A., Klagsbrun, M., Esko, J.D., Leder, P. & Ornitz, D.M. Cell surface, heparin-like molecules are required for binding of basic fibroblast growth factor to its high affinity receptor. *Cell* **64**, 841-8 (1991).

45. Stauber, D.J., DiGabriele, A.D. & Hendrickson, W.A. Structural interactions of fibroblast growth factor receptor with its ligands. *Proc. Natl. Acad. Sci. U. S. A.* **97**, 49-54 (2000).

46. Olsen, S.K., Ibrahimi, O. A., Raucci, A., Zhang, F., Eliseenkova, A. V., Yayon, A., Basilico, C., Linhardt, R. J., Schlessinger, J. & Mohammadi, M. Insights into the molecular basis for fibroblast growth factor receptor autoinhibition and ligand-binding promiscuity. *Proc. Natl. Acad. Sci. U. S. A.* **101**, 935-40 (2004).

47. Mohammadi, M., Dionne, C. A., Li, W., Li, N., Spivak, T., Honegger, A. M., Jaye, M. & Schlessinger, J. Point mutation in FGF receptor eliminates phosphatidylinositol hydrolysis without affecting mitogenesis. *Nature* **358**, 681-4 (1992).

48. Mohammadi, M., Schlessinger, J. & Hubbard, S.R. Structure of the FGF receptor tyrosine kinase domain reveals a novel autoinhibitory mechanism. *Cell* **86**, 577-587 (1996).

49. Li, E. & Hristova, K. Role of receptor tyrosine kinase transmembrane domains in cell signaling and human pathologies. *Biochemistry* **45**, 6241-6251 (2006).

50. Li, E., You, M. & Hristova, K. FGFR3 dimer stabilization due to a single amino acid pathogenic mutation. *J. Mol. Biol.* **356**, 600-612 (2006).

51. You, M., Li, E. & Hristova, K. The achondroplasia mutation does not alter the dimerization energetics of the fibroblast growth factor receptor 3 transmembrane domain. *Biochemistry* **45**, 5551-5556 (2006).

52. You, M., Spangler, J., Li, E., Han, X., Ghoch, P. & Hristova, K. Effect of pathogenic cysteine mutations on FGFR3 transmembrane domain dimerization in detergents and lipid bilayers. *Biochemistry* **46**, 11039-11046 (2007).

53. Chen, L., Krishnamoothy, G., Cui, J., Sept, D. & Hristova, K. Measuring the dimerization of FGFR3 transmembrane domain in cell membrane. *Biophy. J.* 558a-558a (2007).

54. He, L., Horton, W. & Hristova, K. Physical basis behind achondroplasia, the most common form of human dwarfism. *J. Biol. Chem.* **285**, 30103-14 (2010).

55. Chen, F.H., Degnin, C., Laederich, M., Horton, W.A. & Hristova, K. The A391E mutation enhances FGFR3 activation in the absence of ligand. *Biochim. Biophys. Acta, Biomembranes* **1808**, 2045-2050 (2011).

56. Meyers, G.A., Orlow, S.J., Munro, I.R., Przylepa, K.A. & Jabs, E.W. Fibroblast-Growth-Factor-Receptor-3 (Fgfr3) Transmembrane Mutation in Crouzon-Syndrome with Acanthosis Nigricans. *Nat. Genet.* **11**, 462-464 (1995).

57. van Rhijn, B.W., van Tilborg, A. A., Lurkin, I., Bonaventure, J., de Vries, A., Thiery, J. P. van der Kwarst, T. H., Zwarthoff, E. C. & Radvanyi, F. Novel fibroblast growth factor receptor 3 (FGFR3) mutations in bladder cancer previously identified in non-lethal skeletal disorders. *Eur. J. Hum. Genet.* **10**, 819-824 (2002).

58. Shiang, R., Thompson, L. M., Zhu, Y. Z., Church, D. M., Fielder, T. J., Bocian, M., Winokur, S. T. & Wasmuth, J. J. Mutations in the Transmembrane Domain of Fgfr3

Cause the Most Common Genetic Form of Dwarfism, Achondroplasia. *Cell* **78**, 335-342 (1994).

59. Placone, J. & Hristova, K. Direct Assessment of the Effect of the Gly380Arg Achondroplasia Mutation on FGFR3 Dimerization Using Quantitative Imaging FRET. *Plos ONE* **7**(2012).

60. Killian, J.A. Synthetic peptides as models for intrinsic membrane proteins. *FEBS Lett.* **555**, 134-8 (2003).

61. Yano, Y. & Matsuzaki, K. Membrane insertion and dissociation processes of a model transmembrane helix. *Biochemistry* **41**, 12407-13 (2002).

62. Galardy, R.E. & Kortylewicz, Z.P. Synthesis of a Docosapeptide Comprising the Hydrophobic Membrane Spanning Region of Glycophorin-A. *Int. J. Pep. Protein Res.* **26**, 33-48 (1985).

63. Tomita, M. & Marchesi, V.T. Amino-acid sequence and oligosaccharide attachment sites of human erythrocyte glycophorin. *Proc. Natl. Acad. Sci. U. S. A.* **72**, 2964-8 (1975).

64. Smith, S.O., Jonas, R., Braiman, M. & Bormann, B.J. Structure and Orientation of the Transmembrane Domain of Glycophorin-a in Lipid Bilayers. *Biochemistry* **33**, 6334-6341 (1994).

65. Merrifield, R.B., Solid phase peptide synthesis.I. The synthesis of tetrapeptide. *J. Am. Chem. Soc.* 2149-2154 (1963).

66. Hojo, H., Aimoto, S., Polypeptide synthesis using the S-alkyl thioester of a partially protected peptide segment. Synthesis of the DNA-binding domain of c-myb protein (143-193)-NH2. *Bull. Chem. Soc. Jpn.* **64**, 111-117 (1991).

67. Dawson, P.E., Muir, T.W., Clarklewis, I. & Kent, S.B.H. Synthesis of Proteins by Native Chemical Ligation. *Science* **266**, 776-779 (1994).

68. Hirata, R., Ohsumk, Y., Nakano, A., Kawasaki, H., Suzuki, K. & Anraku, Y. Molecular structure of a gene, VMA1, encoding the catalytic subunit of H(+)-translocating adenosine triphosphatase from vacuolar membranes of Saccharomyces cerevisiae. *J. Biol. Chem.* **265**, 6726-33 (1990).

69. Kane, P.M., Yamashiro, C. T., Wolczyk, D. F., Neff, N., Goebl, M. & Stevens, T. H. Protein splicing converts the yeast TFP1 gene product to the 69-kD subunit of the vacuolar H(+)-adenosine triphosphatase. *Science* **250**, 651-7 (1990).

70. Perler, F.B., Davis, E. O., Dean, G. E., Gimble, F. S., Jack, W. E., Neff, N., Noren, C. J.,

Thorner, J. & Belfort, M. Protein splicing elements: inteins and exteins--a definition of terms and recommended nomenclature. *Nucleic Acids Res*. **22**, 1125-7 (1994).

71. Severinov, K. & Muir, T.W. Expressed protein ligation, a novel method for studying protein-protein interactions in transcription. *J. Biol. Chem*. **273**, 16205-9 (1998).

72. Muir, T.W., Sondhi, D. & Cole, P.A. Expressed protein ligation: a general method for protein engineering. *Proc. Natl. Acad. Sci. U. S. A*. **95**, 6705-10 (1998).

Chapter 1

Synthesis of TM-IJM region of FGFR3 with Alexa Fluor 568 C_5-maleimide attached to the C-terminus by Native Chemical Ligation

Protein sample for a biochemical or structural study is commonly prepared using method of molecular biology. *E. coli* and even mammalian cells are employed for protein production. However, a sample required, such as size of the protein or modification on the protein, varies depending on a specific interest or analyzing technique. To expand choices of strategies for sample preparation, methodological development of protein production is important. This is also true for membrane proteins whose preparation is still challenging.

This chapter describes development of technologies that must be useful for molecular characterization or structural analysis on transmembrane (TM) and juxtamembrane (JM) regions of membrane protein. As it has been mentioned in **Introduction**, recent research progress in the field of receptor tyrosine kinase reveals that its intracellular juxtamembrane (IJM) region is functionally important. Studies on the IJM region require two components, the TM region and lipid bilayers, in the system. These two components are what make research on membrane protein even harder. Here, the author introduces and describes, being the TM-IJM region of FGFR3 as a target, a methodology that must be a basis for the next generation of membrane and membrane protein biological chemistry. The technology is introduction of a fluorescence label on a thiol group of cysteine residue with leaving the thiol group of other cyntein residues for native chemical ligation (**Figure 1-1**).

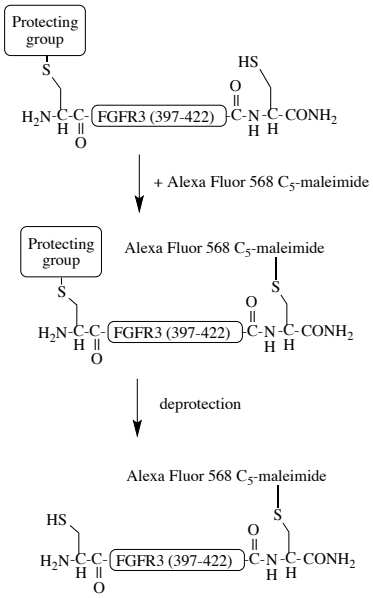

Figure 1-1. Reaction of thiol reactive probe of fluorescence, Alexa Fluor 568 C_5-maleimide, in FGFR3 IJM peptide with protecting the side-chain thiol of N-terminal cysteine

In this thesis, the author focuses on structure and function correlation of the TM-IJM region (**Figure 1-2**). Chemical synthesis of a peptide as such with a length of more than 50 amino acid residues is not a trivial using a general stepwise elongation protocol in the solid phase method. Ligation strategy is commonly used to obtain a peptide that consists of more than 50 amino acid residues as it was mentioned in **Introduction**. As it is shown in **Figure 1-2**, the native sequence of the TM-IJM region contains cysteine at 396. This Cys396 can be used for the ligation site for the native chemical ligation. For preparation of the FGFR3 TM-IJM peptide, the N-terminal building block was designed to be to FGFR3 TM region in residues 367-395 (FGFR3 (367-395)) and the C-terminal building block was designed to be FGFR3 IJM region in residues 396-422

(FGFR3 (396-422)).

```
                                    Asp Glu Ala Gly
371 Ser Val Tyr Ala Gly Ile Leu Ser Tyr Gly
381 Val Gly Phe Phe Leu Phe Ile Leu Val Val
391 Ala Ala Val Thr Leu Cys Arg Leu Arg Ser
401 Pro Pro Lys Lys Gly Leu Gly Ser Pro Thr
411 Val His Lys Ile Sre Arg Phe Pro Leu Lys
421 Arg Gln
```

Figure 1-2. Sequence of FGFR3 TM-IJM region (367-422) Cys396 is written in red and TM region is covered with gray.

One of the aims is to elucidate a molecular characteristic of the IJM region, especially its interaction with lipid bilayer and a lipid molecule such as PIP_2 (**Chapter 2**). Fluorescence spectroscopy is one of the techniques that provide results from which we can make a simple interpretation for what occurs. As a sample, FGFR3 TM-IJM peptide with fluorescence probe at the C-terminus is required. The thiol reactive probe of fluorescence such as Alexa Fluor 568 C_5-maleimide is useful probe to site-specific label in straight-forward manner. As it is mentioned above, FGFR3 TM-IJM sequence has the cysteine residue that natively exists (Cys396) at the boundary between TM and IJM region. Here we may face a problem of not being able to introduce the thiol reactive probe specifically at the C-terminus of the peptide. However, this can be accomplished using ligation. A strategy for the preparation of FGFR3 TM-IJM region with fluorescence probe at the C-terminus is shown in **Figure 1-3**. The point is using a thiazolidine ring to protect the side chain of Cys396 at the introduction of the label.

The ring can simply be opened by treatment of methoxylamine to generate the cysteine side chain[1].

In performing the native chemical ligation, building blocks are mixed in an aqueous buffer. In the current case, one of the expected difficulties is low solubility of the N-terminal building block with the sequence of the TM region due to its high hydrophobicity. Sato and coworkers have reported the synthesis of transmembrane protein by native chemical ligation in presence of detergent to dissolve a building block with transmembrane sequence[2]. Following conditions reported therein, the author examines the synthesis of FGFR3 TM-IJM peptide by native chemical ligation.

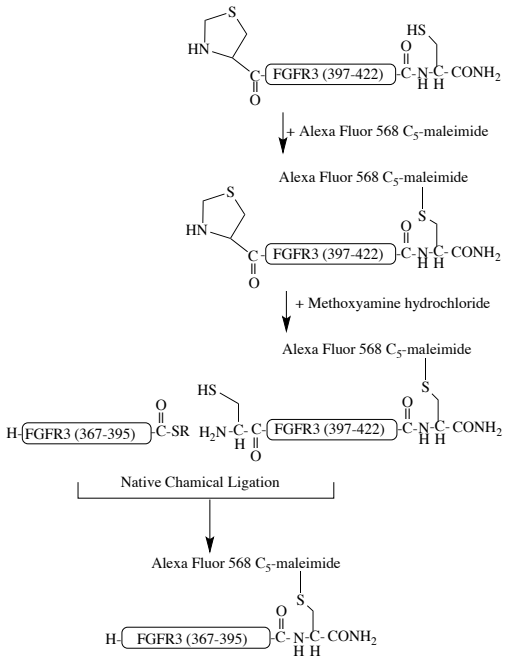

Figure 1-3. Strategy of synthesis of FGFR3 TM-IJM with fluorescence probe at the C-terminus using native chemical ligation

Results and discussion

Overall all scheme for the synthesis of FGFR3 TM-IJM region (367-422) with fluorescence probe, Alexa Fluor 568 C_5-maleimide, attached to the C-terminus is shown in **Scheme 1-1**. The author used the same procedure for preparing three sequences of the TM-IJM region (367-422) with fluorescence probe, Alexa Fluor 568 C_5-maleimide attached to the C-terminus of wild type, G380R and A391E. Result of each step is described.

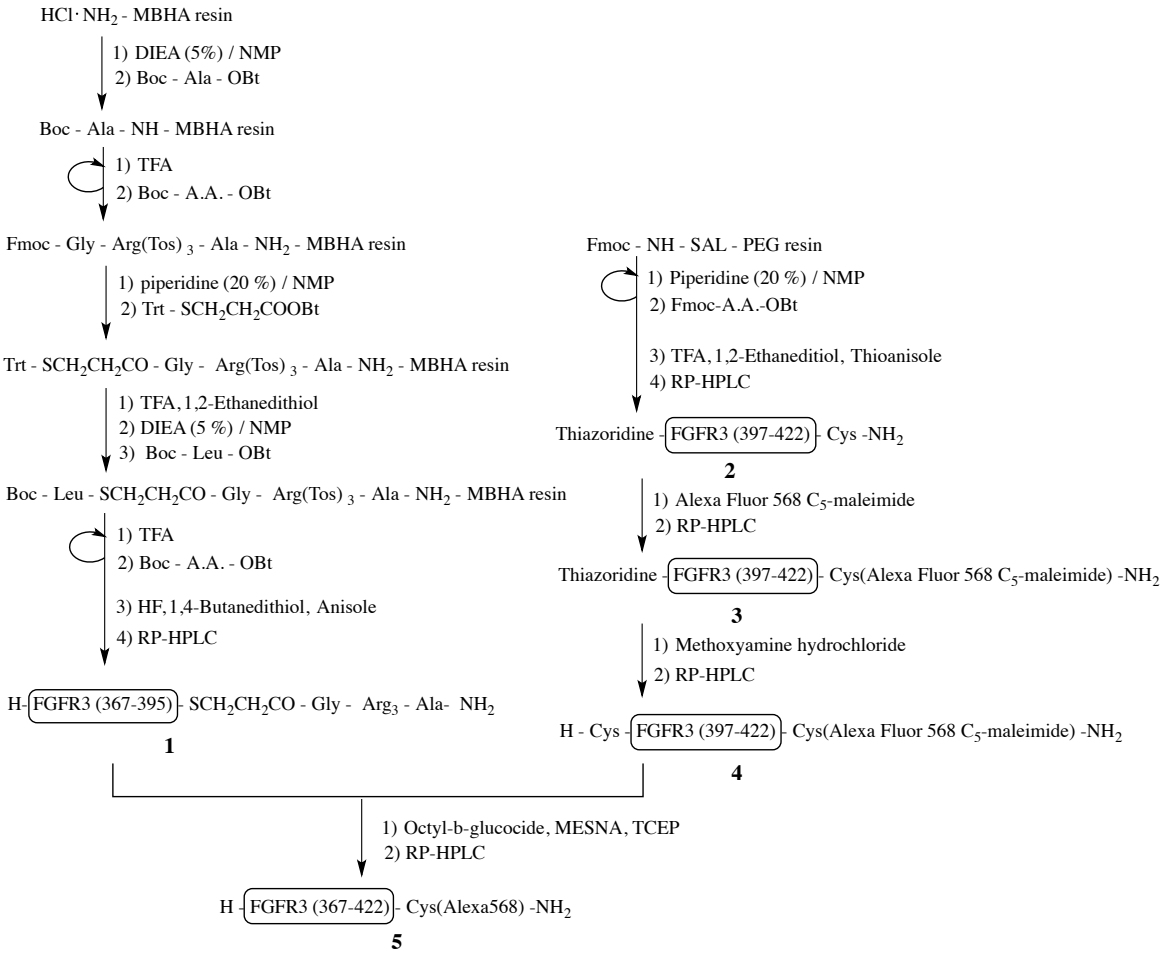

Scheme 1-1. Synthesis of FGFR3 TM-IJM region (367-422) with fluorescence probe, Alexa Fluor 568

- Synthesis of N-terminal building block, FGFR3 TM (367-395) -SCH_2CH_2CO-Gly-Arg_3-Ala-NH_2 (peptide 1), in *t*-Boc chemistry

The synthesis of **peptide 1** was summarized in **Scheme 1-2**. Starting from HCl・NH_2-MBHA resin, Boc-Leu-SCH_2CH_2CO-Gly-Arg(Tos)-Arg(Tos)-Arg(Tos)-Ala-NH_2-MBHA resin was synthesized using the procedure reported by Kawakami et. al.[3] **Peptide 1** was synthesized from Boc-Leu-SCH_2CH_2CO-Gly-Arg(Tos)-Arg(Tos)-Arg(Tos)-Ala-NH_2-MBHA resin using the Boc chemistry. The peptide was cleaved from the resin by treatment with HF.

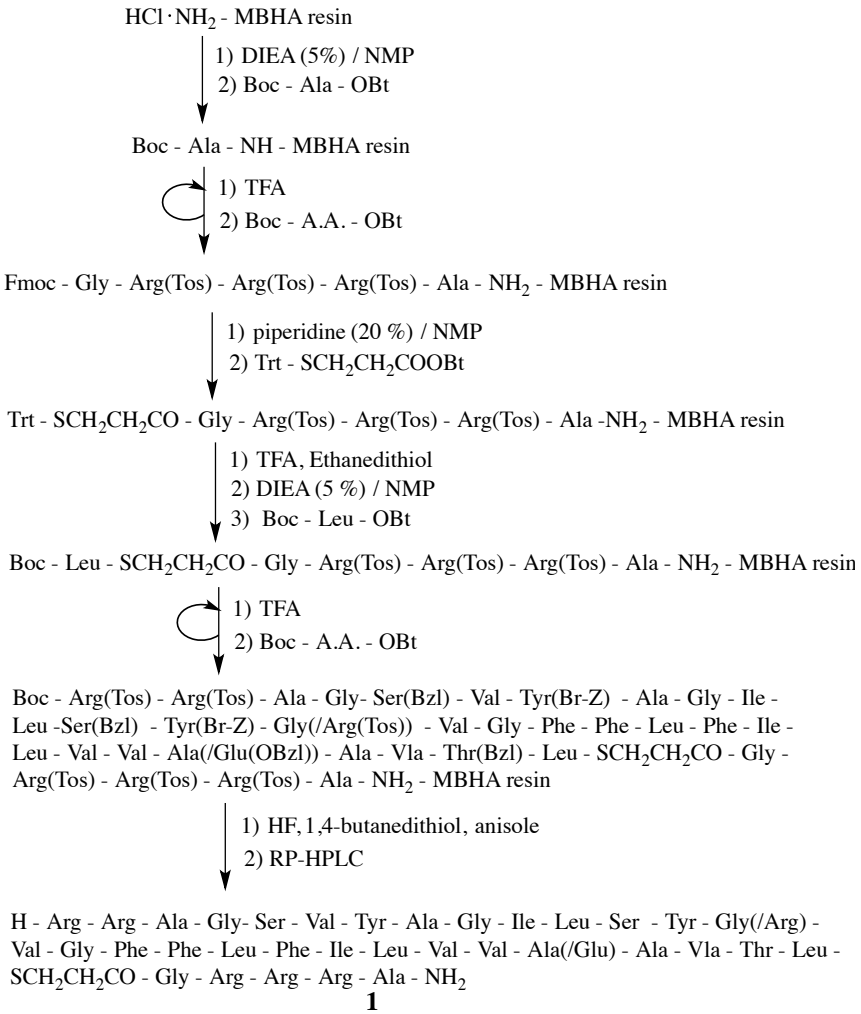

Scheme 1-2. Synthetic scheme of **peptide 1**

The purification was then performed by means of RP-HPLC. Purification using RP-HPLC was performed a linear gradient of formic acid/ water (3: 2) and formic acid/ 1-propanol (4: 1) at a flow rate of 2.00 ml/ min. The RP-HPLC chromatogram for the wild type sequence was shown in **Figure 1-4**. The content of the main peak shown with an arrow on **Figure 1-4** was characterized with MALDI-TOF mass spectrometry. The mass number found agreed with the calculated value for the desired product (wild type found for m/z: 3674.9 calcd for [M+H]+: 3678.3). In other peptides of mutant sequence, G380R and A391E, purifications of RP-HPLC were performed under the same condition with wild type sequence and the mass numbers found from the main peak of RP-HPLC chromatogram also agreed with the calculated value for the desired products (G380R found m/z: 3774.4, calcd for $[M+H]^+$: 3777.4 7015.3 A391E found for m/z: 3739.5, calcd for $[M+H]^+$: 3736.3)

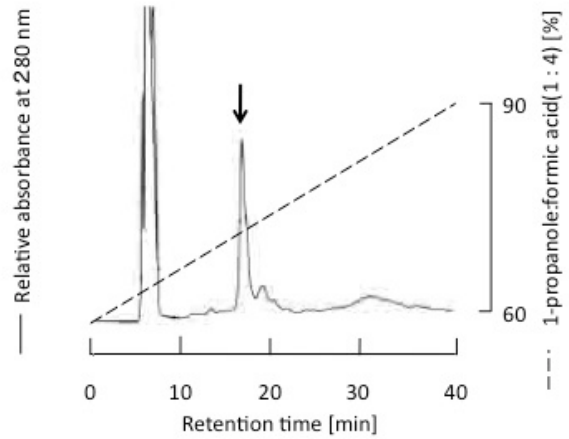

Figure 1-4. RP-HPLC elution profile of the purification of **peptide 1**. The details of conditions are indicated under the chromatogram.

- Synthesis of peptide 2, by the Fmoc Chemistry

The synthesis of **peptide 2** was summarized in **Scheme 1-3**. Starting from NH_2-SAL-PEG resin, the C-terminal segment, FGFR3 IJM (397-422) with thiazoridine ring at the N-terminus was synthesized by Fmoc chemistry. The peptide component was cleaved from the resin by treatment with TFA.

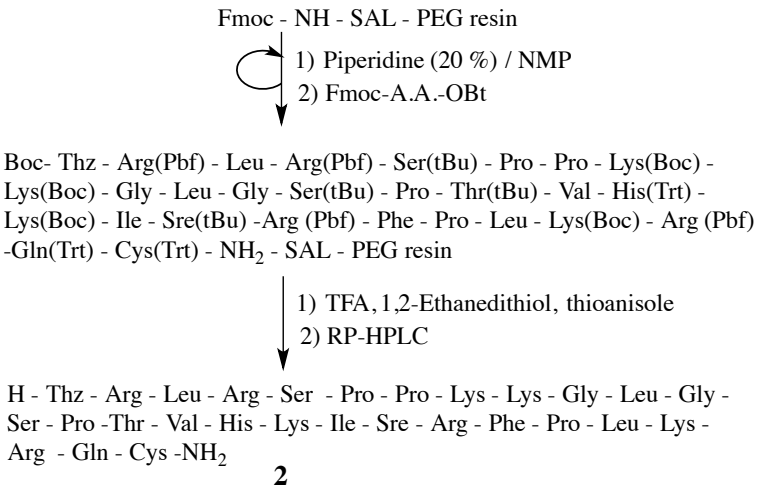

Scheme 1-3. Synthesis of C-terminal building block, **peptide2**

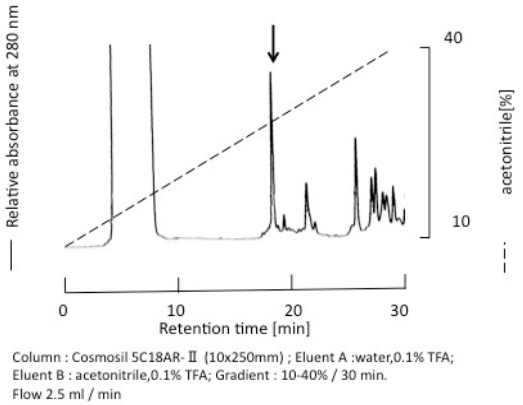

Figure 1-5. RP-HPLC elusion profiles of the purification of **peptide 2**. The details of conditions are indicated under the chromatogram.

Purification by RP-HPLC was performed using a linear gradient of water with 0.1 % TFA and acetonitrile with 0.1 % TFA at flow rate of 2.5 ml/ min. The RP-HPLC

chromatogram was shown in **Figure 1-5**. The content of the main peak shown with an arrow on **Figure 1-5** was characterized with ESI mass spectrometry. The mass number found agreed with the calculated value for the desired product (found m/z: 3072.8, calcd for $[M+H]^+$: 3076.6).

- Introduction of fluorescence probe, Alexa Fluor 568 C_5-maleimide, to cysteine at peptide 2 to obtain peptide 3

Peptide 2 and a thiol reactive probe of fluorescence, Alexa Fluor 568 C_5-maleimide, were mixed in neutral aqueous buffer at 37 °C for 1-2 hours. Purification of **peptide 3** was performed by RP-HPLC. The chromatogram of RP-HPLC was shown in **Figure 1-6**. The mass number of purified peptide was measured by ESI mass spectrometry. (found m/z: 3932.0, calcd for $[M+H]^+$: 3933.5).

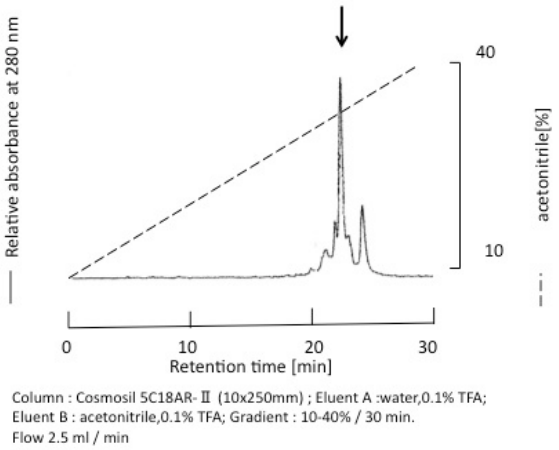

Figure 1-6. RP-HPLC elution profiles of the purification of **peptide 3**. The details of conditions are indicated under the chart.

- Opening the thiazolidine ring to obtain peptide 4 for native chemical ligation

Peptide 3 was mixed with methoxyamine hydrochloride in aqueous buffer at 37 °C for 1-2 hours to obtain **peptide 4**. Purification by RP-HPLC was performed a linear gradient of water with 0.1 % TFA and acetonitrile with 0.1 % TFA at flow rate of 2.5 ml/ min. The chromatogram of purification by RP-HPLC was shown in **Figure 1-7**. The content in the main peak shown with an arrow was characterized by ESI mass spectrometry. The mass number found agreed with the calculated value of the desired product (found m/z: 3920.0, calcd for $[M+H]^+$: 3921.5)

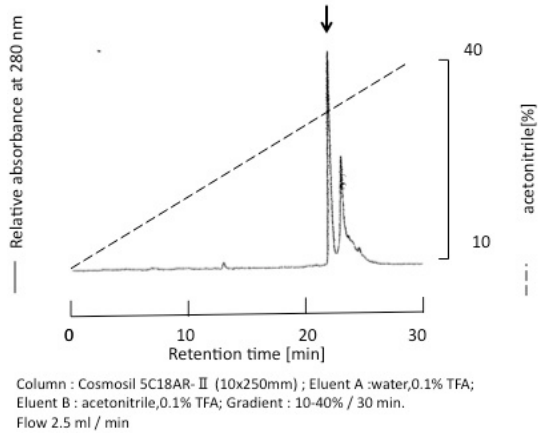

Figure 1-7. RP-HPLC elusion profiles of the purification of **peptide 4**. The details of conditions are indicated under the chromatogram.

- Native chemical ligation for obtaining peptide 5

Native chemical ligation is usually performed in an aqueous solution. A building block with transmembrane sequence must be dissolved with use of detergent. Sato and coworkers has reported that the concentration of the detergent for the ligation reaction is critical and should be maintained below the critical micelle concentration (CMC)[2]. **Peptide 1** was dissolved in aqueous buffer with 15 mM *n*-octyl-β-glucoside (OG) of

which the concentration was less than CMC (20-25 mM). The solution of **peptide 1** with detergent was added **peptide 4**, MESNA and TCEP and stirred at 37 °C overnight. Purification by RP-HPLC was performed using a linear gradient of formic acid/ water (3: 2) and formic acid/ 1-propanol (4: 1) at a flow rate of 2.00 ml/ min. The chromatogram of RP-HPLC for wild type sequence was shown in **Figure 1-8**.

The content in the main peak shown with an arrow was characterized by MALDI-TOF mass spectrometry. The mass number found agreed with the calculated value of the desired product (wild type found m/z: 6896.3, calcd for $[M+H]^+$: 6893.2). In other peptide of mutant sequences, G380R and A391E, the conditions of ligation and purification by RP-HPLC were same with the peptide of wild type sequence and the mass number found from the main peak of RP-HPLC chromatogram agreed with the calculated value of the desired products (G380R found m/z: 7014.8, calcd for $[M+H]^+$: 7015.3 A391E found m/z: 6955.9, calcd for $[M+H]^+$: 6951.2).

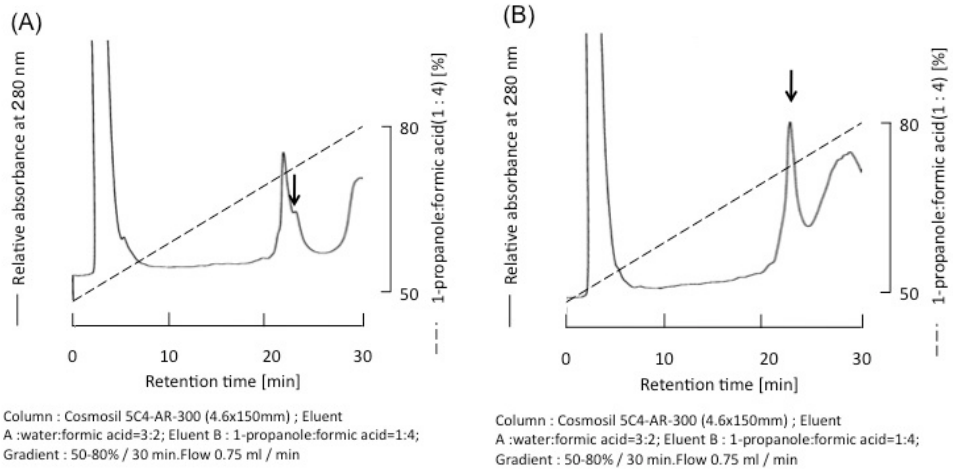

Figure 1-8. The result of ligation to obtain **peptide 5** (A) peptide1 and peptide 4 were mixed in aqueous buffer with 15 mM OG, 25 mM MESNA and 1 mM TCEP. (B) peptide 1 and peptide 4 were mixed in aqueous buffer with 15 mM OG, 25 mM MESNa and 1 mM TCEP at 37 °C after 24 hours . The details of conditions are indicated under the chromatogram.

Material and Methods

HCl・NH_2-MBHA resin and amino acid derivatives were purchased from the Peptide Institute Inc. (Osaka, Japan). Boc-Thz-OH was purchased from Iris Biotwch GmbH (Germany). Fmoc-NH_2-SAL-PGE resin was purchased from Watanabe Chem. Ind., Ltd. (Hiroshima, Japan). Alexa Fluor 568 C_5-maleimide was purchased from Invitrogen (Eugene, OR). The peptide mass number was determined by MALDI-TOF mass spectrometry using a MALDI-TOF MS autoflex™ (Bruker, Germarny). The matrix used was sinapinic acid and peptides were dissolved in a mixture of formic acid and trifluoroethanol.

- Synthesis of peptide 1, by the Boc chemistry

HCl・NH_2-MBHA resin (0.50 mmol, 0.625 g) was treated with 5 % DIEA/ NMP (2x 5 min), washed with NMP (6x 1 min). A solution of Boc-Ala-OH (1.0 mmol), HOBt (0.10 mmol), HBTU (0.9 mmol) and DIEA (2.0mmol) in DMF was added to the resin and stirred for 30 min. After finishing the coupling, the resin was washed with NMP (6x 1 min) and the capping solution of acetic anhydride (10 %) and DIEA (5 %) in NMP (1x 5min) was added. Boc-Ala-NH-MBHA resin was obtained. Boc-Ala-NH-MBHA resin was treated with TFA (2x 1min), washed with DMF (3x flow, 6x 1 min). A solution of Boc-amino acid (1.0 mmol), HOBt (0.10 mmol), HBTU (0.9 mmol) and DIEA (2.0mmol) in DMF was added to the resin and stirred for 30 min. After finishing the coupling, the resin was washed with NMP (6x 1 min) and added the capping solution of acetic anhydride (10 %) and DIEA (5 %) in NMP (1x

5min). These procedures were repeated to obtain Boc-Gly-Arg(Tos)-Arg(Tos)-Arg(Tos)-Ala-NH-MBHA resin. This resin was treated with (2x 1min) and washed with DMF (3x flow, 6x 1 min) and 5 % DIEA/ NMP (2x 5min). Trt-SCH_2CH_2COOH (0.50 mmol), HOBt (0.50 mmol) and DCC (0.50 mmol) in NMP was mixed and the solution was added to the resin. The resin was shaken for 2 hours and washed with NMP (3 x 1 min). The resin was treated with NMP solution containing 10 % acetic anhydride and 5 % DIEA and then washed with NMP (6x 1 min) and DCM (3x 1 min). The resulting resin was treated with TFA containing 2.5 % triisopropylsilane and 2.5 % water (3x 2 min) and washed with DCM (3x 1 min), NMP (1 min) and 5 % DIEA/ NMP (3x 1 min) . The solution of Boc-Leu-OH (1 mmol), HOBt (1 mmol) and DCC (1 mmol) in NMP was added to the resin and shaken for 3 hours to obtain Boc-Leu-SCH_2CH_2CO-Gly-Arg(Tos)-Arg(Tos)-Arg(Tos)-Ala-NH-MBHA resin. Boc -Leu-SCH_2CH_2CO-Gly-Arg(Tos)-Arg(Tos)-Arg(Tos)-Ala-NH-MBHA resin was treated with TFA (2x 1min), washed with DMF (3x flow, 6x 1 min). A solution of Boc-amino acid (1.0 mmol), HOBt (1.0 mmol), HBTU (0.9 mmol) and DIEA (2.0 mmol) in DMF was added to the resin and stirred for 30 min. After finishing the coupling, the resin was washed with NMP (6x 1min) and added the capping solution of acetic anhydride (10 %) and DIEA (5 %) in NMP (1x 5 min). These procedures were repeated to obtain a protected peptide resin corresponding to the sequence of FGFR3 TM (367-395), Boc-Arg(Tos)-Arg(Tos)-Ala-Gly-Ser(Bzl)-Val-Tyr(Br-Z)-Ala-Gly-Ile-Leu-Ser(Bzl)-Tyr(Br-Z)-Gly(/Arg(Tos))-Val-Gly-Phe-Phe-Leu-Phe-Ile-Leu-Val-Val-Ala(/Glu(OBzl))-Ala-Vla-Thr(Bzl)-Leu-SCH_2CH_2CO-Gly-Arg(Tos)-Arg(Tos)-Arg(Tos)-Ala-NH-MBHA

resin. The protected peptide resin (250 mg) was treated with a mixture of anhydrous HF (8.5 mL), anisole (750 μl) and 1,4-butanedithiol (750 μL) at 0 °C for 90 min. After the deprotection, cold ether was added to the mixture and the resulting precipitate was washed with ether and then dissolved in TFA. The solution was passed through a filter and precipitated by the addition of cold ether. The precipitate was washed with ether, and mixed with aqueous acetonitrile and freeze-dried to give the crude powder. Purification was performed on a Cosmosil Columns (10x 250 mm, 5C4-AR-300, Nakalai Tesque), and a linear gradient of formic acid/ water (3: 2) and formic acid/ 1-propanol (4: 1) at a flow rate of 2.00 ml/ min. The crude powder were dissolved in each initial solution of RP-HPLC and injected into the column. The desired product was collected and freeze-dried to obtain **peptide 1**; H-Arg-Arg-Ala-Gly-Ser-Val -Tyr-Ala-Gly-Ile-Leu-Ser-Tyr-Gly(/Arg)-Val-Gly-Phe-Phe-Leu-Phe-Ile-Leu-Val-Val-A la(/Glu)-Ala-Val-Thr-Leu-SCH_2CH_2CO-Gly-Arg-Arg-Arg-Ala-NH_2 (4-6 mg, MAS (MALDI TOF) wild type found m/z: 3674.9 calcd for $[M+H]^+$: 3678.3; G380R found m/z: 3774.4, calcd for $[M+H]^+$: 3777.4 7015.3 A391E found m/z: 3739.5, calcd for $[M+H]^+$: 3736.3)

- Synthesis of peptide 2, by the Fmoc Chemistry

Fmoc-NH_2-SAL-PEG resin (0.24 mmol/g, 1.04 g) was treated with 20 % piperidine/ NMP solution (1x 5 min, 1x 25 min), washed with NMP (6x 1 min). A solution of Fmoc-amino acid (1.0 mmol), HOBt (1.0 mmol), HBTU (0.9 mmol) and DIEA (2.0 mmol) in DMF was added to the resin and stirred for 30 min. After finishing the

coupling, the resin was washed with NMP (6x 1min) and added the capping solution of acetic anhydride (10 %) and DIEA (5 %) in NMP (1x 5 min). These procedures were repeated to obtain a protected peptide resin corresponding to the sequence of FGFR3 IJM region (396-422) with thiazolidine ring at the N-terminus; Boc-Thz-Arg(Pbf)-Leu-Arg(Pbf)–Ser(^{t}Bu)-Pro-Pro-Lys(Boc)-Lys(Boc)-Gly-Leu-Gly-Ser(^{t}Bu)-Pro-Thr(^{t}Bu)-Val-His(Trt)-Lys(Boc)-Ile-Sre(^{t}Bu)-Arg(Pbf)-Phe-Pro-Leu-Lys(Boc)-Arg(Pbf)-Gln(Trt)-Cys(Trt)-NH_2-SAL-PEG resin. The protected peptide resin (250 mg) was treated with a mixture of TFA (4.1 ml), thioanisole (250 μl), phenol (250 mg), ethanedithiol (125 μL) and water (250 μl) at room temperature for 2 hours 30 min. After the deprotection, cold ether was added to the mixture and the resulting precipitate was wash with ether and then dissolved in aqueous acetonitrile. The solution was passed through a filter and freeze-dried to give the crude powder. Purification was performed on a Cosmosil Column (10x 250 mm, 5C18-AR-ll, Nakalai Tesque), and a linear gradient of water with 0.1 % TFA and acetonitrile with 0.1 % TFA at flow rate of 2.5 ml/ min. The crude powder was dissolved in water with 70 % TFA and injected into the column. The desired product was collected and freeze-dried to obtain **peptide 2**; Thz-Arg-Leu-Arg–Ser-Pro-Pro-Lys-Lys-Gly-Leu-Gly-Ser-Pro-Thr-Val-His-Lys-Ile-Sre-Arg-Phe-Pro-Leu-Lys-Arg-Gln-Cys-NH_2 (MAS(ESI) found m/z: 3072.8, calcd for $[M+H]^+$:3076.6).

- Introduction of fluorescence probe, Alexa Fluor 568 C_5-maleimide, to peptide 2 and obtain peptide 3

The purified **peptide 2** (1 mmol) and Alexa Fluor 568 C_5-maleimide (1 mmol) were mixed in 50 mM phosphate buffer pH 7.5 (3 mL) containing TCEP (1 mmol) at 37 °C

for 2 hours. Purification was performed on a Cosmosil Column (10x 250 mm, 5C18-AR-ll, Nakalai Tesque), and a linear gradient of water with 0.1 % TFA and acetonitrile with 0.1 % TFA at flow rate of 2.5 ml/ min to **peptide 3**; Thz-Arg-Leu-Arg–Ser-Pro-Pro-Lys-Lys-Gly-Leu-Gly-Ser-Pro-Thr-Val-His-Lys-Ile-Sre -Arg-Phe-Pro-Leu-Lys-Arg-Gln-Cys(Alexa Fluor 568 C_5-maleimide)-NH_2 (MAS (ESI) found m/z: 3932.0, calcd for $[M+H]^+$: 3933.5)

- Opening the thiazolidine ring to obtain the C-terminnal building block, peptide 4, for native chemical ligation

Peptide 3 (1 mmol) and methoxyamine hydrochloride (75 μmol) were mixed in 50 mM acetate buffer pH 4.0 (3 mL) at 37 °C for 2 hours. Purification was performed on a Cosmosil Column (10x 250 mm, 5C18-AR-ll, Nacalai Tesque), and a linear gradient of water with 0.1 % TFA and acetonitrile with 0.1 % TFA at flow rate of 2.5 ml/ min to obtain **peptide 4**;H-Cys-Arg-Leu-Arg–Ser-Pro-Pro-Lys-Lys-Gly-Leu-Gly-Ser-Pro-Thr-Val-His-Lys-Ile-Sre-Arg-Phe-Pro-Leu-Lys-Arg-Gln-Cys(Alex Fluor 568 C_5-maleimide) -NH_2 (MAS (ESI) found m/z: 3920.0, calcd for $[M+H]^+$: 3921.5)

- Native chemical ligation for obtaining peptide 5

Peptide 1 (0.1 μmol) and **peptide 4** (0.1 μmol) were dissolved in 50 mM phosphate buffer pH7.5 (100 μL) including MESNA (2.5 μmol) and OG (1.5 μmol). The solution was stirred at 37 °C overnight. The reaction was monitored by RP-HPLC (4.6x 150 mm, 5C4-AR-300, Nakalai Tesque), and a linear gradient of formic acid/ water (3: 2) and formic acid/ 1-propanol (4: 1) at a flow rate of 0.75 ml/ min. Purification was performed on a Cosmosil Columns (10x 250 mm, 5C4-AR-300,

Nakalai Tesque), and a linear gradient of formic acid/ water (3: 2) and formic acid/ 1-propanol (4: 1) at a flow rate of 2.00 ml/ min. Peaks were collected and freeze-dried. As a result, a desired peptide was obtained; H-Arg-Arg-Ala-Gly-Ser-Val-Tyr-Ala-Gly-Ile-Leu-Ser-Tyr-Gly(/Arg)-Val-Gly-Phe-Phe-Leu-Phe-Ile-Leu-Val-Val-Ala(/Glu)-Ala-Val-Thr-Leu-Cys-Arg-Leu-Arg–Ser-Pro-Pro-Lys-Lys-Gly-Leu-Gly-Ser-Pro-Thr-Val-His-Lys-Ile-Sre-Arg-Phe-Pro-Leu-Lys-Arg-Gln-Cys(Alexa Fluor 568 C_5-maleimide)-NH_2 (MAS (MALDI) wild type found for m/z: 6896.3, calcd for [M+H]+: 6893.2; G380R found for m/z: 7014.8, calcd for [M+H]+: 7015.3 A391E found for m/z: 6955.9, calcd for [M+H]+: 6951.2)

1. Bang, D. & Kent, S.B. A one-pot total synthesis of crambin. *Angew. Chem. Int. Ed. Engl.* **43**, 2534-8 (2004).
2. Sato, T., Saito, Y. & Aimoto, S. Synthesis of the C-terminal region of opioid receptor like 1 in an SDS micelle by the native chemical ligation: effect of thiol additive and SDS concentration on ligation efficiency. *J. Pep. Sci.* **11**, 410-416 (2005).
3. Kawakami, T., Hasegawa, K. & Aimoto, S. Synthesis of a phosphorylated polypeptide by a thioester method. *Bull. Chem. Soc. Jpn.* **73**, 197-203 (2000).

Chapter 2

Effect of the transmembrane helix tilt to the intracellular juxtamembrane region release from the membrane

The negatively charged interacellular juxtamembrane (IJM) region of EGFR and ErbB2/Neu, that are member of receptor tyrosine kinases (RTKs), interacts with positively charged lipid bilayer surface[1-4]. Also, the model that the IJM region is released from membrane for activation was established[4,5] as described in **Introduction**. The interaction between IJM region and membrane suggests important factor for the activation mechanism of RTKs. In this chapter, we worked on the structural analysis of the transmembrane-interacellular juxtamambene (TM-IJM) region in fibroblast growth factor receptor 3 (FGFR3). To get insight on the "active structure", the author performed structural analyses on sequences of G380R and A391E. These mutations are known to be activating mutations in the TM region of FGFR3 as describe in **Introduction**. The structure of TM-IJM peptide of wild type, G380R and A391E in lipid bilayer are compared using spectroscopic experiments, such as solid-state NMR, fluorescence experiments and polarized FT-IR. The role of TM-IJM region for activity is discussed from the structural comparison.

Results

- TM helix breaks at the membrane boundary

To obtain information on the secondary structure for the TM-IJM boundary region, we obtained ^{13}C spectra of TM-IJM peptides in the wild type and G380R sequence

containing specific backbone ^{13}C labels at the putative TM-IJM boundary. TM-IJM peptide contains a single ^{13}C=O labeled amino acid at Leu388 and Leu395. Leu388 is considered to be located in the middle of the TM region whereas Lue395 is at the TM-IJM boundary. The spectra were obtained at a spinning frequency of 12.5 kHz and a temperature at -50 °C.

The carbonyl ^{13}C chemical shifts are sensitive to the secondary structure. Saito and Naito have correlated chemical shifts from solid-state NMR studies of fibrous and membrane proteins and have found that in helical secondary structure, carbonyl carbons exhibit chemical shifts in the range of 173-176 ppm, while in random coil and β-strand structure they are in the range of 168-172 ppm[6].

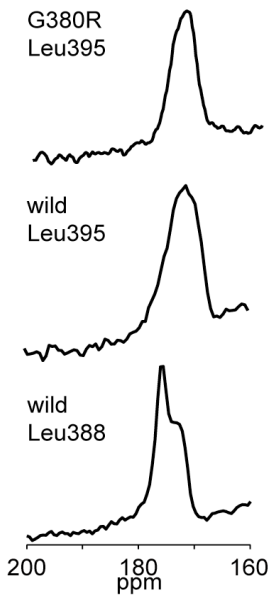

Figure 2-1. ^{13}C=O spectra of solid-state NMR for the secondary structure of FGFR3 TM region.

Chemical shifts for ^{13}C=O from Leu388, Leu395 on the wild type and Leu395 on G380R sequence were 175.8, 172.8 and 172.0 ppm respectively. For Leu388 in the

middle of the TM region, ^{13}C on the backbone C=O showed typical chemical shift for being in α-helical structure. Contrarily, Leu395 located at the boundary region was suggested to be in extended structure. Considering the fact that two consecutive prolines exist at two residues away towards the C-terminus, the IJM region is expected to be in random extended structure.

- The IJM sequence of the TM-IJM (G380R) and TM-IJM (A391E) peptides is not associated with membrane surface

The IJM sequence of FGFR3 has some positively charged residues that would be expected to bind to the negatively charged surface of plasma membrane. Previous studies by McLaughlin and co-workers showed that model polylysine peptides with 3 and 5 residues bind to model membranes having 33 % negative charged and 100 mM monovalent salt with free energy of 3 and 5 kcal/ mol[7]. Our system with 4 positive charges, 23 % negatively charged lipids (POPC/ POPS = 10/ 3) and 100 mM monovalent salt is similar. Furthermore, it was shown that the addition of polyvalent PIP_2, but not monovalent PS lipids, leads to aggregation of positively charged peptides on the membrane surface[8] .

Figure 2-2 (A) presents the results of fluorescence experiments on the IJM sequence with the fluorescence label, Alexa Fluor 568, attached to the C-terminus. The peptides were added to large unilamellar vesicles (LUVs) formed by extrusion. The vesicles were composed of POPC and POPS in a 10:3 molar ratio. PIP_2 was incorporated into the vesicles by mixing with a solution of PIP_2 micelles and the fluorescence intensity of

the Alexa Fluor 568 label was measured as a function of the amount of PIP_2 in the bilayer. McLaughlin and coworkers have shown that PIP_2 monomers can be incorporated into the outer leaflet of pre-formed vesicles by exposing them to micelles of PIP_2[8]; fluorescence correlation spectroscopy measurements showed PIP_2 diffuses with other lipids in the membrane (giant unilamellar vesicles) after incorporation.

The fluorescence emission band and the excitation absorption band of Alex Fluor 568 were at 604 nm and 568 nm, respectively. The fluorescence intensity decreased with the addition of PIP_2. We interpret this as quenching of the Alexa Fluor 568 as the JM peptides aggregate on the membrane surface. Similar results were observed for the positively charged JM peptides corresponding to the Neu receptor[4].

Secondly, similar experiments were performed for TM-IJM peptides reconstituted into LUVs composed of POPC and POPS in a 10:3 molar ratio. The TM-IJM peptides with the fluorescence label, Alexa Fluor 568, at the C terminus were synthesized by native chemical ligation as explained in **Chapter 1**. **Figure 2-2 (B)** shows that the fluorescence intensity of TM-IJM (wild type) decreased with the addition of PIP_2. The change in the fluorescence intensity of TM-IJM (wild type) shown in **Figure 2-2 (B)** can be attributed to the effect of PIP_2 on the IJM region. It was assumed that the IJM region of the wild type sequence should be bound to the membrane so as to be affected by PIP_2, which was partitioned into the membrane. This interpretation can be supported by the fact that similar results were obtained for the isolated IJM sequence (**Figure 2-2 (A)**). Furthermore, the structural cause for the decrease in the fluorescence intensity was considered to be the formation of TM-IJM association,

which led to self-quenching of the dye. In contrast, no nominal change was observed in the fluorescence intensity of TM-IJM (G380R) and TM-IJM (A391E) with the addition of PIP_2, as shown in **Figures 2-2 (C)** and **(D)**, respectively. The lack of fluorescence changes in the TM-IJM (G380R) and TM-IJM (A391E) sequences can be attributed to a lack of IJM-IJM association, suggesting that the IJM sequence has partitioned off of the membrane.

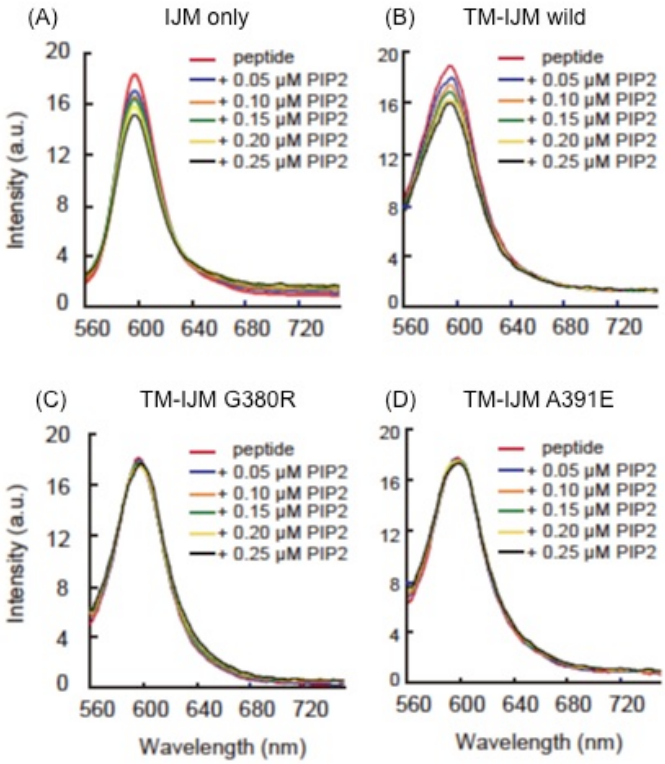

Figure 2-2. Fluorescence spectra of IJM, TM-IJM wild type, TM-IJM (G380R) and TM-IJM (A391E). The influence of PIP_2 on IJM-IJM interaction was measured for the TM-IJM sequences of the isoated IJM region **(A)** and the TM-IJM peptide with wild type **(B)**, G380R **(C)** and A391E **(D)**, respectively.

We further confirmed the interaction of the IJM region with the acidic membrane by tryptophan fluorescence experiments. Binding and insertion of tryptophan into the

hydrophobic membrane results in a blue-shift of the fluorescence emission band. We chemically synthesized FGFR3 peptides (367-433) corresponding to the wild type sequence and G380R and A391E mutants and having tryptophan residue at the C-terminus. The peptides were reconstituted into lipid bilayers composed of POPC/POPS (10/ 3). Here we set the peptide-to-lipid ratio to 1:100 (or even up to 1:50) as opposed to that of 1:1000 for observing the fluorescence from Alexa Fluor 568. In our system, the high ratio was required to overcome the effect of light scattering from the lipid vesicles. We have confirmed that addition of PIP_2 to the system reduces the fluorescence intensity from mutant sequence (data not shown), in agreement with the results on Alexa Fluor 568 fluorescence at a 1:1000 molar ratio. **Figure 2-3** shows results of the fluorescence measurements from tryptophan for each sequence. Intensities are normalized to the fluorescence intensity value measured at the wavelength of the emission maximum. In the system without PIP_2, we observed only a small difference in value of λ_{max}. The difference becomes distinct with the addition of PIP_2 to vesicles. The spectrum from the wild type sequence is blue-shifted 7 nm relative to the mutant sequences.

Our result suggests that the IJM region is released from the membrane with the activating mutations, G380R and A391E, in the TM region.

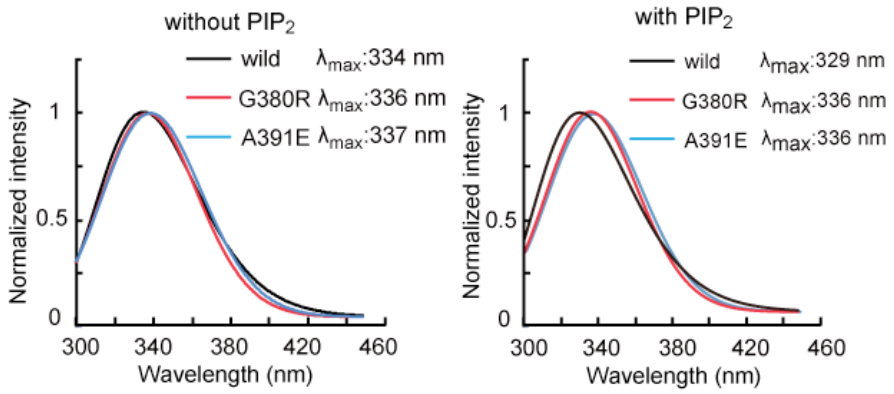

Figure 2-3. Tryptophan fluorescence spectra of wild type TM-IJM with G380R and A391E mutants. Spectra show the fluorescence from the prptides reconstituted into the membrane with PIP_2 (on the left) and without PIP_2 (on th right)

- G380R and A391E mutation induce a change in TM helix orientation

The fluorescence experiments described above argue that the Alexa Fluor 568 and tryptophan labels at the C-terminus of the IJM region are in different environments in the G380R and A391E mutants compared to the wild-type peptide. In this section, investigation was made to see whether there is a change in the orientation of the TM portion of the peptide in these mutants using polarized FT-IR spectroscopy.

The TM-IJM (wild type), TM-IJM (G380R) and TM-IJM (A391E) peptides were reconstituted into POPC/ POPS (10/ 3) or DMPC/ DMPG (10/ 3) vesicles, and the vesicles were aligned on an attenuated total reflection (ATR) plate for polarized FT-IR measurements. **Figure 2-4** shows the deconvoluted polarized FT-IR spectra of these sequences. The peak at 1657 cm^{-1} corresponds to α-helical structure within the TM sequence. The dichroic ratio of each sequence is also shown in the figure. The values presented are the average results from multiple measurements (>3). The

dichroic ratios of the TM-IJM (G380R) and TM-IJM (A391E) peptides were higher than that of the TM-IJM (wild type) peptide, suggesting that the TM helices with the pathogenic mutations are less tilted than that of the TM helix of the wild type peptide. This tendency was observed for measurements in both POPC/ POPS and DMPC/ DMPG membranes.

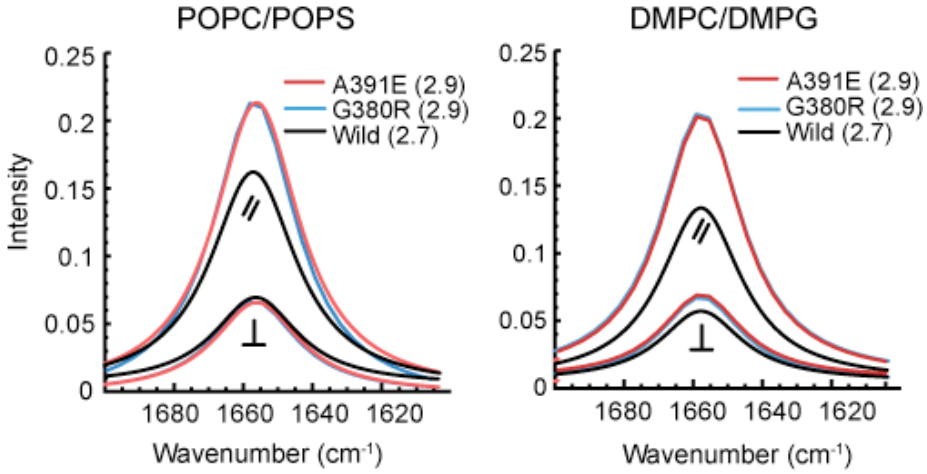

Figure 2-4. Polaried FT-IR spectra of wild type TM helix with G380R and A391E in lipid bilayer. The three TM-IJM peptides were reconstituted into POPC/ POPS (10: 3) or DMPC/ DMPG (10: 3), membranes, and FT-IR spectra were obtained with light polarlized parallel (//) or perpendicular (⊥) to the membrane normal. The frequency of the amide I band at ~1657 cm^{-1} is characteristic of the α-helix.

Then, an investigation was made to examine whether, for the wild type, the orientation of the TM helix affected the release of the IJM region from the membrane. The TM helix tilt was changed by reconstituting the TM-IJM (wild type) peptide into lipid bilayers with different thicknesses, which were varied by using lipids with different acyl chain lengths. It has been shown that the tilt angle of model TM peptides (WALP and KALP) decreased as membrane thickness increases due to the hydrophobic mismatch

[9,10]. In addition, it has been shown that tilt angle of the TM helix of the platelet-derived growth factor receptor, another RTK, decreases as the membrane thickness increase. For these experiments, the TM-IJM (wild type) peptide was reconstituted into different bilayers containing POPC, 1, 2-dioctadecanoyl-*sn*-glycero-3-phosphocholine (C18) or 1, 2-dinonadecanoyl-*sn*-glycero-3-phosphocholine (C19), respectively. In each case, POPS (23 %) was added to maintain a negatively charged membrane surface. The dichroic ratio was observed to increase with an increase in the length of the acyl chain (C18: 2.8, C19: 3.3). Thickness of lipid bilayers used are expected to be 27 Å for POPC[11], 29.5 Å for C18 and 30.5 Å for C19[12]. A dichroic ratio of 3.3 corresponds to helix tilt angle of ~ 20 ° and a crossing angle between helices in a dimer of ~ 40 °a, a typical value of helices in a left-handed coilded-coil geometry.

In order to examine the effect of the TM helix orientation on the interaction of the IJM sequence with the membrane surface, we performed similar experiments as described above to determine whether PIP_2 affected the fluorescence intensity of the Alexa 568 incorporated at the C-terminus of the TM-IJM (wild type) peptide. The results are shown in **Figure 2-5**. For the POPC vesicles, the fluorescence intensity decreased upon the addition of PIP_2 (**Figure 2-5 (A)**); for the C18 vesicles, the intensity first increased with the initial addition of PIP_2 and then decreased with additional PIP_2 (**Figure 2-5 (B)**). The decrease in the intensity of POPC and C18 vesicles can be attributed to the association of IJM strands and interactions of the vesicles with PIP_2. However, for the C19 vesicles, the intensity was not responsive to the addition of PIP_2 (**Figure 2-5 (C)**), indicating that no interaction occurred between the IJM region and

PIP_2 and further suggesting that the IJM sequence was released from the membrane. A simple conclusion that can be drawn from the polarized FT-IR and fluorescence experiments is that for FGFR3, the IJM region is released from the membrane as the TM helix orientation is shifted closer to the membrane normal.

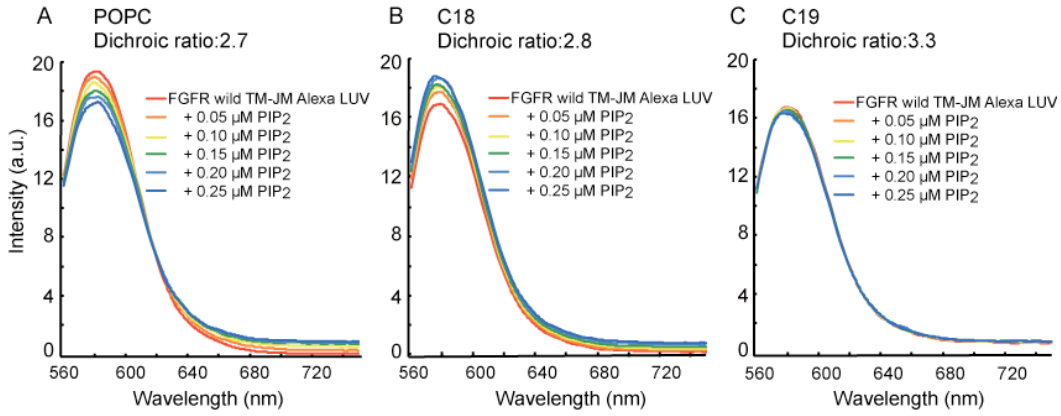

Figure 2-5. Fluorescence experiments with the TM helix orientation. The TM-IJM peptide in the wild type was reconstituted into POPC **(A)**, C18 **(B)** and C19 **(C)** with 23 % POPS. The influence of PIP_2 on IJM interactions was measured.

Discussion

FGFR3 is similar to the ErbB2/Neu receptor in that the mutation of specific hydrophobic residues in the TM sequence arginine to or glutamate can result in receptor activation. In the case of the ErbB2/Neu receptor, the V664E mutation shifts the monomer-dimer equilibrium toward the dimeric state, and the specific orientation of the helices in the receptor dimer facilitates the partitioning of the positively charged IJM sequence from membrane surface[4]. In the FGFR3, there are two clinically important mutations (G380R and A391E) that lead to receptor activation. The extensive studies

of Hristova and coworkers have indicated that these mutations influence TM helix interactions in FGFR3. In fact, the A391E mutation in FGFR3 appears analogous to the V664E mutation in the ErbB2/Neu receptor, in that both strengthen the association of helices in a specific active orientation. The major finding in our current studies is that these mutations leads to similar changes in the orientation of the TM helices and the spectral changes on probes attached to the IJM domain. These changes were interpreted to partitioning of the IJM region from the membrane surface.

The IJM region has long been recognized as an important regulatory site in RTKs[13]. The IJM sequences are highly positively charged. The positive charge not only serves as the stop sequence of TM helices into cell membrane, but it also terminates the TM helix. McLaughlin and others have shown that such highly positively charged sequences can bind to negatively charged membrane surfaces and serve to sequester the highly negatively charged phosphoinositide, PIP_2[1-3]. While PIP_2 can act as second messenger in signal transduction, and has been associated with EGFR activity[14], PIP_2 was used in the current studies as a way to measure membrane association of the IJM region of the FGFR3. Another regulatory mechanism involving the IJM region of RTKs is the interaction with calcium calmodulin, which is known to bind to the IJM region of EGFR[15]. Calcium calmodulin interacts with the IJM region of EGFR and facilitates its dissociation from the membrane, which in turn increase the trans phosphorylation of its interacelluar domain[1]. Phosphorylation typically occurs within the activation loop or C-terminus of the kinase domain. However, can also occur with the IJM region itself. The studies presented here and previously provide insight into

how the IJM can function in regulatory role[4].

For the FGFR subfamily, there is only limited structural information concerning how the extracellular domain is coupled to the intracellular kinase domain. Here, characterization was made for the IJM region of FGFR3 in order to see if there are parallels with the ErbB receptor sub family. The IJM region from FGFR3 binds to the acidic membrane containing PIP_2. Importantly, this region is released from the membrane with an activating mutation, G380R or A391E, in the TM sequence.

The positively charged sequence of the IJM region suggests that electrostatic interactions are essential for both membrane binding and release. In the ErbB system, we modulated the helix orientation with the V664E mutation and engineered dimers[4]. We assume that in the G380R and A391E peptides, the TM and IJM regions are in active configurations. As mentioned above, the dimerization propensity differs between these mutant sequences[16,17], and consequently the mechanism for activity enhancement without ligand binding cannot be fully explained on the basis of dimerization alone. It is possible that there are two different changes in the TM region (induced by the two different activating mutations), which lead to similar changes on the intracellular side of membrane. Here the observation was made that decrease in the helix tilt angle relative to the membrane normal (*i.e.* the helices "stand up" in the membrane) as a common feature for these two mutant sequences. Furthermore, for the wild type sequence, it was found that the decrease of the TM helix tilt allows the release of the IJM region from the membrane. Based on the similar observations regarding the TM helix tilt and the IJM release in the two FGFR3 mutant peptides, a proposal can be

made such that the orientation of the TM helices in active full-length receptor dimers contributes to release of the IJM region, allowing asymmetric interactions to occur between the intracellular kinase domain.

The mechanism for release of the IJM region from the membrane has still not been elucidated. One important consideration is whether the IJM sequence is simply a helical extension of the TM helix or whether the secondary structure breaks at the TM-IJM boundary and the IJM sequence is unstructured. Solid-state NMR experiments on peptides containing 1-^{13}C labeled amino acids show that the TM helix breaks ta the TM-IJM boundary and suggest that IJM region is unstructured (**Figure 2-1**). A similar observation was made for the ErbB2/Neu receptor peptides. In the wild type peptides (and for the isolated IJM peptides), the unstructured, positively charged IJM sequence interacts electrostatically with the negatively charged membrane surface[2,4]. A proposal can be made that the TM helices become less tilted in the membrane, or dimerization propensity is increased with A391E mutation[16], the TM helices are brought together on the C-terminal side of the membrane. This change would bring the positively charged ends of the helices into closer proximity and result in repulsion between the IJM positive charges. It can be suggested that this might facilitate the release of the IJM region from the membrane.

Material and Methods

^{13}C-labeled amino acids were purchased from Cambridge Isotope Laboratories (Andover MA). *n*-octyl-β-D-glucoside was obtained form Nacalai Tesque (Kyoto

Japan). Lipids ware obtained from Avanti Polar Lipids (Alabster, AL).

- Synthesis of FGFR3 TM-IJM peptide

FGFR3 TM-IJM peptides were synthesized by method of Fmoc or Boc solid phase peptide synthesis. Synthesis of FGFR3 TM-IJM peptides with Alexa Fluor 568 at the C-terminus was performed according to the procedures mentioned in Chapter 2-1. FGFR3 TM-IJM peptides with tryptophan at the C-terminus were synthesized using automated microwave peptide synthesizer, Blue Liberty (CEM corporation). Purification of FGFR3 TM-IJM peptide was performed by RP-HPLC. In RP-HPLC, the solutions of water/ formic acid (3: 2) and formic acid/ 1-propanol (4: 1) were used (ref). The mass number of purified peptides was measured by MALDI-TOF mass spectrometry.

- Reconstitution of peptides into lipid bilayers for NMR experiments

The FGFR3 receptor peptides were co-solubilized with DMPC, DMPG and n-octyl-β-D-glucoside in chloroform and trifluoroethanol. The peptide: lipid molar ration was 1: 50; the molar ratio between DMPC: DMPG was 10:3. The solution was incubated for 90 min at 37 °C, after which the solvents were removed under a stream of argon gas and then under vacuum. MES buffer (50 mM MES, 50 mM NaCl, 5 mM DTT, pH 6.2) was added to the solid from the previous step and mixed at 37 °C for 6 h. The n-octyl-β-D-glucoside was removed by dialysis. The reconstituted membrane were pelleted and loaded into NMR rotors.

- Solid-state NMR spectroscopy

Solid-state NMR magic angle spinning (MAS) experiments were performed in Varian Infinity-plus 500, 600 and 700 spectrometers operated at 11.74 T, 14.09 T and 16.44 T, respectively (Palo Alto CA). Broadband triple resonance MS probe for 3.2 mm and 4.0 mm rotors were used. For ^{13}C=O-observe experiments, the MAS frequency was maintained at 12.5 kHz and single pulse excitation was employed with a 5 μs 90 ° pulse length, followed by a 10 μs delay before data acquisition. The probe temperature was maintained at -50 °C.

- Fluorescence Spectroscopy

Fluorescence experiments were carried out on a Hitachi F-2500 fluorescence spectrophotometer. After the reconstitution, vesicles were formed by extrusion through a 200 nm polycarbonate filter. POPC and POPS (or other wise mentioned) in the ratio of 10: 3 were employed for the lipid bilayers in the fluorescence experiments. The peptide-to-lipid ratio depends on the fluorescence probe that we used. The ratio was set to 1: 1000 for observing the fluorescence from Alexa Fluor 568. For experiments measuring the fluorescence from tryptophan, the ratio was set to 1: 100. The lipid concentration was 200-250 μM in MOPS buffer (1 mM MOPS, 0.1 M KCl, pH 7.0). For experiments with PIP_2, the PIP_2 was introduced into the membrane by addition of PIP_2 micelles to the vesicle solution [8]. The PIP_2 concentration ranged from 0.05 μM to 4 μM, corresponding to PIP_2-to-peptide ratios of 1: 50- 2: 1. For

experiments monitoring Alexa Fluor 568, excitation wavelength was 568 nm. For monitoring tryptophan fluorescence, the excitation wavelength was 295 nm.

- Polarized FT-IR spectroscopy

Polarized attenuated total reflection (ATR) FT-IR spectra were obtained on a Hitachi FT-730 spectrometer. Membranes containing FGFR3 TM-IJM peptides (~ 1-2 mg) were layered on a germanium internal reflection element using a slow flow of nitrogen gas directed at an oblique angle to the IR plate to form an oriented multilamellar lipid-peptide film. 1000 scans were acquired and averaged for each sample at a resolution of 4 cm^{-1}. Absorption of polarized light by the amide I bound yields the dichroic ratio defined as a ratio of absorption intensity for parallel relative to perpendicular polarized light. From the dichroic ratio, we estimated the tilte angle of the TM helix relative to the membrane normal based on the method described by Smith and coworkers using a value of 41.8 for angle α between the helix director and the transition-dipole moment of the amide I vibrational mode [18,19]. For our ATR FT-IR experiment, the amount of lipid used per experiment is ~4 mg. Considering the area of the ATR plate covered (~500 mm^2), the films on the plate in our experiments are assumed to be greater than ~10 μm. For calculating dichroic ratio, the thick film limit is applicable [20]. Equations that we have been using for the calculating the dichroic ratios are based on this assumption.

1. McLaughlin, S., Smith, S.O., Hayman, M.J. & Murray, D. An electrostatic engine model for autoinhibition and activation of the epidermal growth factor receptor (EGFR/ErbB) family. *J. Gen. Physiol.* **126**, 41-53 (2005).
2. Sato, T., Pallavi, P., Golebiewska, U., McLaughlin, S. & Smith, S.O. Structure of the membrane reconstituted transmembrane-juxtamembrane peptide EGFR(622-660) and its interaction with Ca2+/calmodulin. *Biochemistry* **45**, 12704-12714 (2006).
3. Sengupta, P., Bosis, E., Nachliel. E., Gutman, M., Smith, S. O., Mihályné, G., Zaitseva, I. & McLaughlin, S. EGFR Juxtamembrane Domain, Membranes, and Calmodulin: Kinetics of Their Interaction. *Biophys. J.* **96**, 4887-4895 (2009).
4. Matsushita, C., Tamagaki, H., Miyazawa, Y., Aimoto, S., Smith, S. O. & Sato, T. Transmembrane helix orientation influences membrane binding of the intracellular juxtamembrane domain in Neu receptor peptides. *Proc. Natl. Acad. Sci. U. S. A.* **110**, 1646-1651 (2013).
5. Endres, N.F., Das, R., Smith, A. W., Arkhipov, A., Kovacs, E., Huang, Y., Pelton, J. G., Shan, Y., Shaw, D. E., Wemmer, D. E., Groves, J. T. & Kuriyan, J. Conformational Coupling across the Plasma Membrane in Activation of the EGF Receptor. *Cell* **152**, 543-556 (2013).
6. Saito, H.T., Satoru; Naito, Akira. Empirical Versus N On Empirical Evaluation Of Secondary Structure Of Fibrous And Membrane Proteins By Solid-State NMR: A Practical Approach. *Annu. Rep. NMR Spectros.* **36**, 79-121 (1998).
7. BenTal, N., Honig, B., Peitzsch, R.M., Denisov, G. & McLaughlin, S. Binding of small basic peptides to membranes containing acidic lipids: Theoretical models and experimental results. *Biophys. J.* **71**, 561-575 (1996).
8. Golebiewska, U., Gambhir, A., Hangyás-Mihályné, G., Zaitseva, I., Rädler, J. & McLaughlin, S. Membrane-bound basic peptides sequester multivalent (PIP2), but not monovalent (PS), acidic lipids. *Biophys. J.* **91**, 588-599 (2006).
9. Ozdirekcan, S., Rijkers, D.T., Liskamp, R.M. & Killian, J.A. Influence of flanking residues on tilt and rotation angles of transmembrane peptides in lipid bilayers. A solid-state 2H NMR study. *Biochemistry* **44**, 1004-12 (2005).
10. Strandberg, E., Ozdirekcan, S., Rijkers, D. T., van der Wel, P. C., Koeppe, R. E. 2nd, Liskamp, R. M. & Kippian, J. A. Tilt angles of transmembrane model peptides in oriented and non-oriented lipid bilayers as determined by 2H solid-state NMR. *Biophys. J.* **86**, 3709-21 (2004).

11. Muhle-Goll, C., Hoffmann, S., Afonin, S., Grage, S. L., Polyansky, A. A., Windisch, D., Zeitler, M., Bürck, J. and Ulrich, A. S. Hydrophobic matching controls the tilt and stability of the dimeric platelet-derived growth factor receptor (PDGFR) beta transmembrane segment. *J. Biol. Chem.* **287**, 26178-86 (2012).
12. Lewis, B.A. & Engelman, D.M. Lipid bilayer thickness varies linearly with acyl chain length in fluid phosphatidylcholine vesicles. *J. Mol. Biol.* **166**, 211-7 (1983).
13. Hubbard, S.R. Juxtamembrane autoinhibition in receptor tyrosine kinases. *Nat. Rev. Mol. Cell Biol.* **5**, 464-71 (2004).
14. Michailidis, I.E. et al. Phosphatidylinositol-4,5-bisphosphate regulates epidermal growth factor receptor activation. *Pflugers Arch.* **461**, 387-397 (2011).
15. Martin-Nieto, J. & Villalobo, A. The human epidermal growth factor receptor contains a juxtamembrane calmodulin-binding site. *Biochemistry* **37**, 227-236 (1998).
16. Li, E., You, M. & Hristova, K. FGFR3 dimer stabilization due to a single amino acid pathogenic mutation. *J. Mol. Biol.* **356**, 600-612 (2006).
17. You, M., Li, E. & Hristova, K. The achondroplasia mutation does not alter the dimerization energetics of the fibroblast growth factor receptor 3 transmembrane domain. *Biochemistry* **45**, 5551-5556 (2006).
18. Smith, S.O., Smith, C., Shekar, S., Peersem, O., Zilliox, M. & Aimoto, S. Transmembrane interactions in the activation of the Neu receptor tyrosine kinase. *Biochemistry* **41**, 9321-9332 (2002).
19. Liu, W., Eilers, M., Patel, A.B. & Smith, S.O. Helix packing moments reveal diversity and conservation in membrane protein structure. *J. Mol. Biol.* **337**, 713-729 (2004).
20. Bechinger, B., Ruysschaert, J.M. & Goormaghtigh, E. Membrane helix orientation from linear dichroism of infrared attenuated total reflection spectra. *Biophys. J.* **76**, 552-563 (1999).

Chapter 3

Insight on the dimer structure of the tranesmembrane region of FGFR3

In the previous chapter, it was revealed that the tilt of the transmembrane (TM) helix relative to the membrane modulates the interaction of the intracellular juxtamembrane (IJM) region and the membrane, which also suggests that the TM region has an active role in the receptor function. One of the earliest studies that shed light on the role of the TM region for receptor tyrosine kinase (RTK) function is a sturdy by Bargmann and coworkers who found a constitutively active and oncogenic mutation (V664E) in the TM region of ErbB2[2,3]. Later on, Smith and coworkers reported that the side chain of glutamic acid residue from the V664E mutation form an inter-helical hydrogen bound to stabilize its active dimer structure[4]. Furthermore, Stern and coworkers have reported that changing the relative position of $VE_{664}G$ within the TM region promotes weak dimerization but not transformation[5]. These findings suggest that the dimerization of TM region is not enough for the receptor to perform its function. The authors, in our previous study on the structure of TM-IJM region of ErbB2/Neu[6], found that the IJM region release from the relative orientation of TM helices that are in dimer. The evidences suggest that, also for FGFR3, to get insight on a possible role of the TM region, the orientation of the TM helices mentioned in the previous chapter must be discussed in a context of dimer structure. In this chapter, the author focuses on dimer interface of the TM region of FGFR3.

Results

- Deuterium NMR provides a probe of helix dimerization, orientation and motion

The FT-IR spectra indicate a distinct change in helix tilt between the TM-IJM peptides corresponding to inactive wild type and active mutant sequences. Hristova and coworkers have shown that the TM sequences of the wild type, G380R and A391E peptides of FGFR3 have the potential to dimerize in lipid bilayers[7-9]. Comparison of dimerization between the wild type and G380R peptides showed that the G380R mutation did not alter the monomer-dimer equilibrium in lipid bilayers[7]. In contrast, comparison of the wild type and A391E mutant peptides showed that the A391E mutation stabilizes the TM dimers[8].

Deuterium magic angle spinning (MAS) NMR spectroscopy provides a simple method to probe helix dimerization, orientation and motion[10]. The intensities of the spinning side bands in the deuterium MAS spectrum are sensitive to molecular motion. Leucine with a single deuterated methyl group at the end of its long side chain is highly mobile in TM helices when facing the surrounding lipids and is relatively more constrained when being packed within a dimer interface, suggesting its use as a probe of the interface for interacting TM helices. The author used deuterium NMR here to see if the changes observed by fluorescence and FT-IR between wild type and mutants are observed (i.e. that the wild-type sequence is different from G380R and A391E, but that G380R and A391E are similar).

Deuterated luecine was introduced to positions 385 and 388 of the TM-IJM sequences of the wild type, G380R and A391E peptides. These leucines are in the middle of the

TM region. The spectra are shown in **Figure 3-1**.

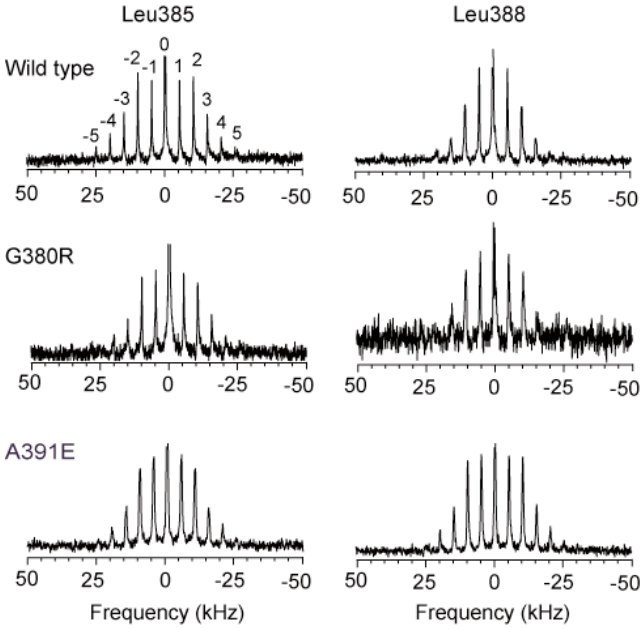

Figure 3-1. Deuterium MAS spectra of 5, 5, 5-^{2}H Leu385 and Leu388 incorporated to the wild type, G380R and A391E FGFR3 TM-IJM peptides. Wild type (top), G380R (middle), A391E (bottom) peptides with deuterium labeling at Leu385 (left column) and Leu388 (right column) were reconstituted into DMPC: DMPG vesicles. The spectra were obtained at 25 °C with a MAS frequency of 5 kHz. The MAS sidebands are labeled as ±1, ±2, ±3 etc., from the center band at a frequency of 0 kHz. The spacing between side bands corresponds to the MAS frequency of 5 kHz.

Distinct differences can be observed between the spectra of Leu385 and Leu388 in TM-IJM (wild-type). The line shape of Leu385 is broader than Leu388, which corresponds to decreased mobility of the Leu385 side chain. (Differences in the breadth of the line shape are reflected, for example, in the intensity of the -2 and 2 spinning side bands.) The line shape of Leu385 is typical of that observed when the labeled leucine is in a dimer interface[6,11]. In contrast, the -2 and 2 side bands in the

spectrum of Leu388 are much less intense than the -1 and 1 side bands indicating that Leu388 is more mobile, consistent with an orientation facing the lipids.

Comparison of the spectra of the TM-IJM (wild-type) peptide with those of TM-IJM (G380R) and TM-IJM (A391E) peptides shows that for Leu385 the side band pattern is slightly narrower than that observed for Leu385 in TM-IJM (wild type). One possibility is that the mutant peptides have a different dimerization interface from the wild type. A second possibility is that the association of the IJM sequence to the membrane surface influences rotational diffusion of the TM dimer. The rotational diffusion of the TM dimer can be increased with the IJM regions being released from the membrane resulting in a narrower overall line width.

- Dipolar assisted rotational resonance (DARR) experiment provide a distance information for TM dimer associating site

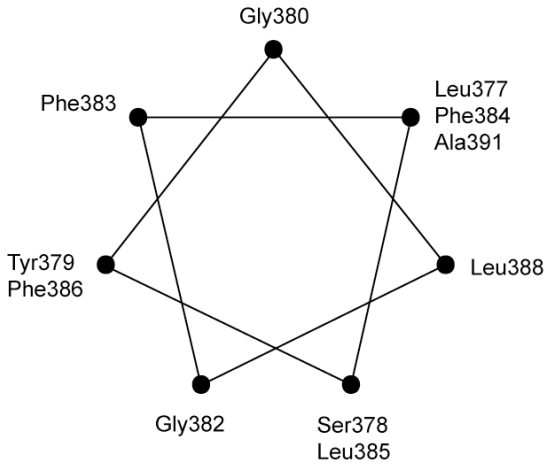

Figure 3-2. Helical wheel diagram for TM region of FGFR3 with key residues.

The line shape of Leu385 in **Figure 3-1** is typical of that observed when the labeled

leucine is in a dimer interface. A simple helical wheel diagram in **Figure 3-2** suggests that Ser378 and Gly382 may also be located in the dimer interface. The Ser378-Gly382 interface is consistent with the small amino acid motif originally identified in the N-termini of RTKs by Sternberg and Gullick[12]. The dimer interface predicted here agrees with the one obtained from MD simulation by Sansom and coworkers on FGFR3[13].

To test whether this Ser378-Gly382 mediates inter-helical association, solid-state NMR experiments were undertaken of the membrane-reconstituted FGFR3 TM-IJM region in the wild-type sequence. **Figure 3-3** presents the results of NMR measurements between FGFR3 TM-IJM peptide at Gly382. Two peptide were synthesized for these experiments; one with 1-^{13}C-Gly and the second with 2-^{13}C-Gly. The two peptides were reconstituted in a 1:1 molar ratio. The observation of a ^{13}C…^{13}C crosspeak (shown with arrow in **Figure 3-3**) in the 2D dipolar assisted rotational resonance (DARR) NMR experiment indicates that these carbons are in contact, consistent with the formation of TM dimer. Together with deuterium MAS data from the previous section and this 2D spectrum suggest that the wild-type TM-IJM peptides dimerize helix using an interface mediated by Ser378-Gly382-Leu385.

For TM helices dimer in the wild type sequence of FGFR3, a high-resolution structure is reported by Arsiniev and coworkers [1]. The structure was obtained with the TM helices in detergent micelles. One of the important features is that the dimer interface contains Gly380, which contradicts with the results mentioned above. Here author investigated to see whether this contact reported by Arsiniev and coworkers can be

found in the conditions used in this study.

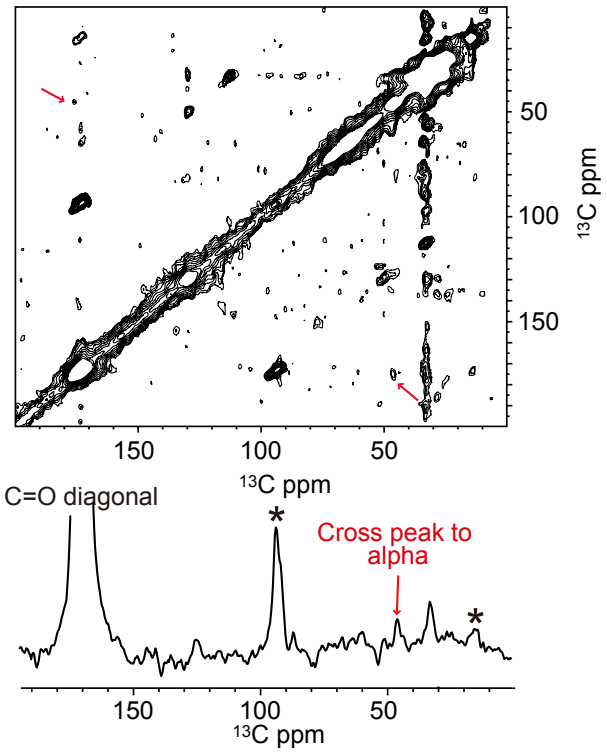

Figure 3-3. 2D DARR NMR measurments between FGFR3 TM-IJM peptide labelse at Gly382. Two peptides were synthesized for these experiments; one with 1-^{13}C-Gly and the second with 2-^{13}C-Gly. The two peptides were reconstituted in a 1: 1 molar ratio. The 2D spectrum is shown in the top. A slice from ^{13}C=O diagonal peak is shown in the bottom. Stars show spinning side bands. Cross peaks are shown in red arrows.

Figure 3-4 presents the results of NMR measurements between FGFR3 TM-IJM peptides labeled at Gly382. Two peptides were synthesized for these experiments; one with 1-^{13}C-Gly and the second with 2-^{13}C-Gly. The two peptides were reconstituted in a 1: 1 molar ratio. No ^{13}C…^{13}C crosspeak in the 2D DARR spectrum indicates that these carbons are not in contact.

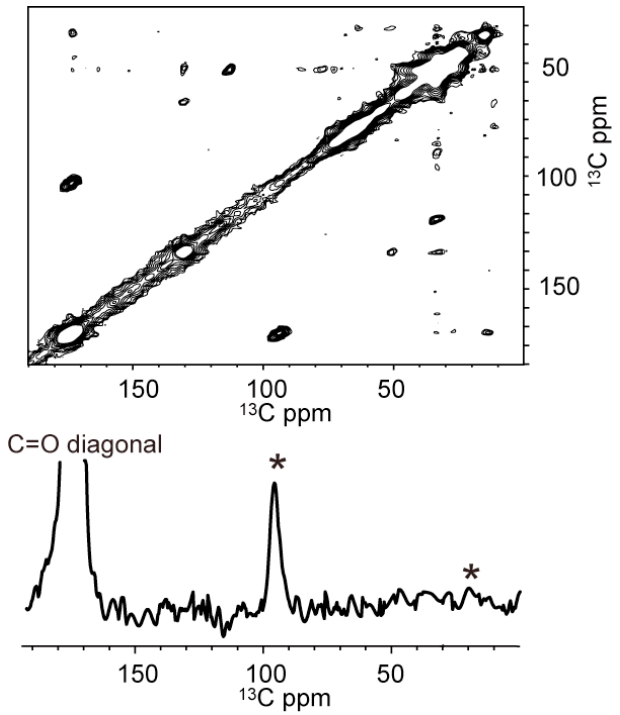

Figure 3-4. 2D DARR NMR measurments between FGFR3 TM-IJM peptide labelse at Gly380. Two peptides were synthesized for these experiments; one with 1-^{13}C-Gly and the second with 2-^{13}C-Gly. The two peptides were reconstituted in a 1: 1 molar ratio. The 2D spectrum is shown in the top. A slice from ^{13}C=O diagonal peak is shown in the bottom. Stars show spinning side bands.

Discussion

In **Figure 3-5 (A)**, a model derived from structural constraints mentioned above for the TM dimer structure is shown. This dimer structure is one of the structures calculated from the simulation program CHI [14]. The deuterium NMR results suggest that Leu385 lies in the dimer interface of the wild type receptor. Furthermore, DARR results suggest that Gly382 is participated in the inter-helical contact in TM helices in dimer. Also it was found that Gly380 was not involved in an inter-helical contact. This

orientation is consistent with the presence of the Ser378-Gly382 sequence at the N-terminus of the TM helix. An SxxxA motif has been shown to mediate dimerization of TM region of ErbB2 [15], while both GxxxG [16] and SxxxS [17] sequences have been implicated in TM dimerization. The dimer interface that we predict agrees with the one obtained for FGFR3 by Sansom and coworkers using molecular dynamics [13]. However, the result does not agree with the interface observed in the high-resolution structure reported by Arsiniev and coworkers rather (**Figure 3-5 (B)**) [1], it corresponds to the activated configuration that they proposed. The difference from our structure may arise from their use of detergent micelles as a membrane mimicking media. Micelles and bilayers may impose different constraints on the tilt angles of the interacting helices and hence the lowest energy interface.

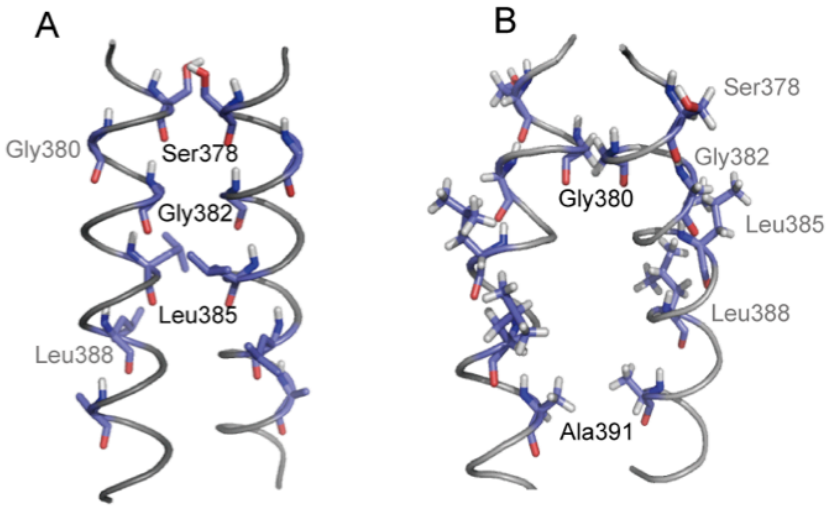

Figure 3-5. Structural models for TM dimer of FGFR3. A: The model established in the authors's study, B: Structrue derived from Arsiniev and coworkers[1].

Material and methods

Sample preparation was performed as described in the previous chapter.

- Solid-state NMR spectroscopy

Solid-state NMR magic angle spinning (MAS) experiments were performed on Varian Infinity-plus 500, 600 and 700 spectrometers operated at 11.47 T, 14.09 T and 16.44 T, respectively (Palo Alto CA). For deuterium-observe experiments, the magic angle spinning (MAS) frequency was maintained at 5 kHz and single pulse excitation was employed with a 5 ms 90 ° pulse length, followed by a 10 ms delay before data acquisition. A total of ~600,000 transients were averaged for each spectrum. For Carbon 13 observe experiments, solid state NMR MAS experiments were performed on JEOL RESONANCE 500 spectrometers operated at 11.74 T. Broadband triple resonance MAS probes for 3.2 mm rotor was used. The ramped amplitude cross polarization contact time was 2 ms. Two-pulse phase-modulated decoupling was used during the evolution and acquisition periods with a field strength of 72 kHz. Internuclear $^{13}C\ldots^{13}C$ distance constraints were observed from 2D DARR NMR experiments using a mixing time of 500 ms. The sample temperature was maintained at 213 K.

1. Bocharov, E.V., Lesovoy, D. M., Goncharuk, S. A., Goncharuk, M. V., Hristova, K. & Arseniev, A. S. Structure of FGFR3 Transmembrane Domain Dimer: Implications for Signaling and Human Pathologies. *Structure* **21**, 2087-2093 (2013).
2. Bargmann, C.I., Hung, M.C. & Weinberg, R.A. Multiple Independent Activations of the Neu Oncogene by a Point Mutation Altering the Transmembrane Domain of P185. *Cell* **45**, 649-657 (1986).
3. Bargmann, C.I. & Weinberg, R.A. Increased Tyrosine Kinase-Activity Associated with the Protein Encoded by the Activated Neu Oncogene. *Proc. Natl. Acad. Sci. U. S. A.* **85**, 5394-5398 (1988).
4. Smith, S.O., Smith, C.S. & Bormann, B.J. Strong hydrogen bonding interactions involving a buried glutamic acid in the transmembrane sequence of the neu/erbB-2 receptor. *Nat. Struct. Biol.* **3**, 252-258 (1996).
5. Burke, C.L., Lemmon, M.A., Coren, B.A., Engelman, D.M. & Stern, D.F. Dimerization of the p185(neu) transmembrane domain is necessary but not sufficient for transformation. *Oncogene* **14**, 687-696 (1997).
6. Matsushita, C., Tamagaki, H., Miyazawa, Y., Aimoto, S., Smith. S. O. & Sato, T. Transmembrane helix orientation influences membrane binding of the intracellular juxtamembrane domain in Neu receptor peptides. *Proc. Natl. Acad. Sci. U. S. A.* **110**, 1646-1651 (2013).
7. You, M., Li, E. & Hristova, K. The achondroplasia mutation does not alter the dimerization energetics of the fibroblast growth factor receptor 3 transmembrane domain. *Biochemistry* **45**, 5551-5556 (2006).
8. Li, E., You, M. & Hristova, K. FGFR3 dimer stabilization due to a single amino acid pathogenic mutation. *J. Mol. Biol.* **356**, 600-612 (2006).
9. Soong, R., Merzlyakov, M. & Hristova, K. Hill Coefficient Analysis of Transmembrane Helix Dimerization. *J. Memb. Biol.* **230**, 49-55 (2009).
10. Liu, W., Crocker, E., Constantinescu, S.N. & Smith, S.O. Helix packing and orientation in the transmembrane dimer of gp55-P of the spleen focus forming virus. *Biophys. J.* **89**, 1194-1202 (2005).
11. Sato, T., Pallavi, P., Golebiewska, U., McLaughlin, S. & Smith, S.O. Structure of the membrane reconstituted transmembrane-juxtamembrane peptide EGFR(622-660) and its interaction with Ca2+/calmodulin. *Biochemistry* **45**,

12704-12714 (2006).

12. Sternberg, M.J. & Gullick, W.J. A sequence motif in the transmembrane region of growth factor receptors with tyrosine kinase activity mediates dimerization. *Protein Eng*. **3**, 245-8 (1990).
13. Reddy, T., Manrique, S., Buyan, A., Hall, B. A., Chetwynd, A. & Sansom, M. S. Primary and Secondary Dimer Interfaces of the Fibroblast Growth Factor Receptor 3 Transmembrane Domain: Characterization via Multiscale Molecular Dynamics Simulations. *Biochemistry* **53**, 323-32 (2014).
14. Adams, P.D., Arkin, I.T., Engelman, D.M. & Brunger, A.T. Computational searching and mutagenesis suggest a structure for the pentameric transmembrane domain of phospholamban. *Nat. Struct. Biol*. **2**, 154-62 (1995).
15. Mendrola, J.M., Berger, M.B., King, M.C. & Lemmon, M.A. The single transmembrane domains of ErbB receptors self-associate in cell membranes. *J. Biol. Chem*. **277**, 4704-12 (2002).
16. Russ, W.P. & Engelman, D.M. The GxxxG motif: a framework for transmembrane helix-helix association. *J. Mol. Biol*. **296**, 911-9 (2000).
17. Adamian, L. & Liang, J. Interhelical hydrogen bonds and spatial motifs in membrane proteins: polar clamps and serine zippers. *Proteins* **47**, 209-18 (2002).

Chapter 4

Semi-synthesis of FGFR3 [FGFR3 (23-407)] and FGFR3 Y373C [FGFR3 Y373C (23-422)]

Ligand binding to the extracellular domain (ECD) is a common initial step for the activation of RTK. As mentioned in **Introduction**, our research is aimed at elucidating the activation mechanism of FGFR3 and the missing part to be uncovered is structural change in the TM and JM regions for the activity. A challenge in this thesis is semi-synthesis of FGFR3 [FGFR3 (23-407)] and FGFR Y373C [FGFR3 Y373C (23-422)], which must provide a way to proceed to the structural biophysical research by enabling introduction of specific labels to the TM-JM region. The concept of semi-synthesis is shown in **Figure 4-1**.

Semi-synthesis is to ligate expressed protein fragment to chemically synthesized

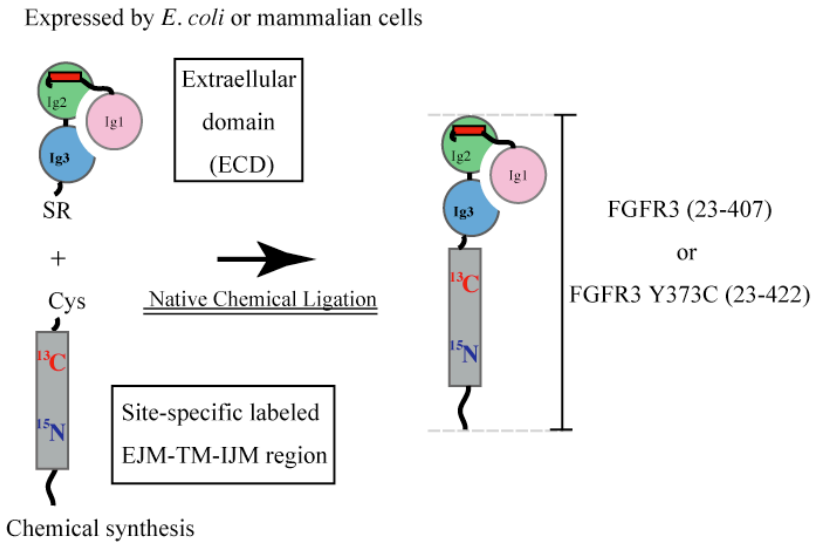

Figure 4-1. Concept of semi-synthesis of FGFR3 (23-407) and FGFR3 Y373C (23-422)

counterpart [1, 2]. In our research, the ECD with a certain modification for the purpose of ligation is prepared by expression system either in *E. coli* or mammalian cells. The

TM-IJM region is chemically synthesized or biologically expressed depending on a method of structural characterization. Desirable labels and/or modifications can be incorporated to the TM-IJM region. In this section, semi-synthesis of FGFR3 [FGFR3 (23-407)] and FGFR Y373C [FGFR3 Y373C (23-422)] is described. Details on the preparation of building blocks and the ligation reaction are reported.

Results

Overall scheme for semi-synthesis of FGFR3 [FGFR3 (23-407)] and FGFR Y373C [FGFR3 Y373C (23-422)] is shown in **Scheme 4-1**.

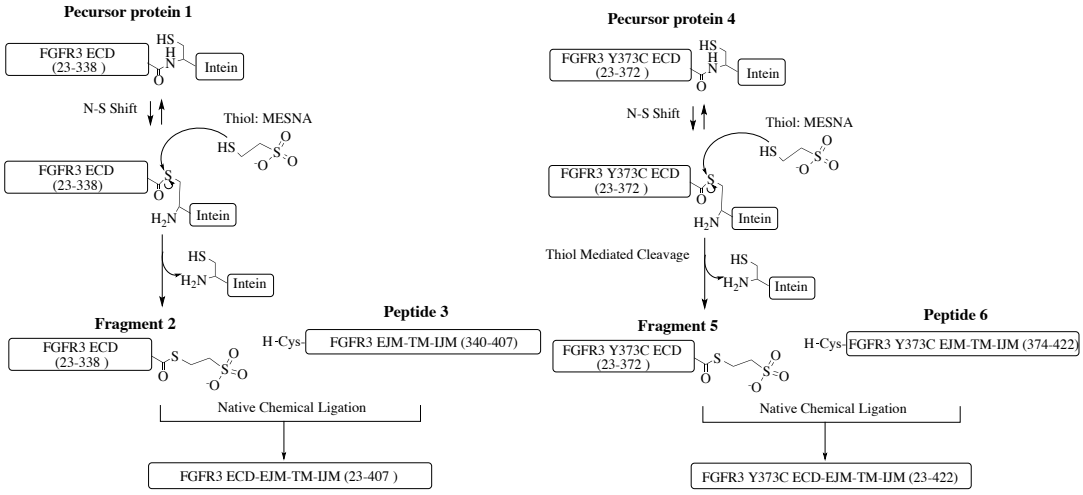

Scheme 4-1. Semi-synthesis of FGFR3 ECD-EIJM-TM-IJM (23-407) and FGFR3 Y373C ECD-EIJM-TM-IJM (23-422) The products in each step were named **(Precursor protein1, Fragment 2, Peptide 3, Precursor protein 4, Fragment 5 and Peptide 6)**.

N-terminal building blocks, **fragment 2** and **5**, were obtained by the thiol-induced cleavage of **"precursor" protein 1** and **4**, which were expressed by *E.coli* or mammalian cells. The thiol-induced cleavage occurs with folding of the intein including protein 1 as described in **Introduction**. The C-terminal building blocks, **peptide 3** and **6**, were obtained by the chemical synthesis. **Fragment 2** and **peptide 3**,

fragment 5 and **peptide 6** were ligated respectively by native chemical ligation in aqueous buffer including detergent to obtain the semi-synthesized receptor. Results for each steps are described.

Semi-synthesis of FGFR3 (23-407) using protein expression by *E. coli*

- Preparation of N-terminal building block, fragment 2, with expression by *E. coli*

pTXB1 FGFR3 ECD His tag vector was subcloned to express the precursor protein of FGFR3 ECD, FGFR3 ECD (23-338)-*Mxe gyrA* intein-chitin binding domain (CBD)-His tag (**precursor protein 1**), by *E. coli*. The construct of vector was shown in **Figure 4-2**.

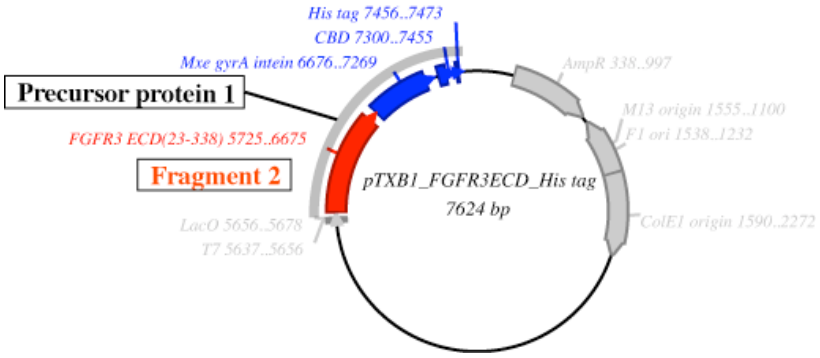

Figure 4-2. Construct of pTXB1 FGFR3 ECD with His tag vector

The vector was transformed to *E. coli* BL21 (DE3) pLysS to obtain **precursor protein 1**. **Precursor protein 1** was found in the cell pellet. The pellet was dissolved in 100 mM Tris-HCl (pH8.0) buffer containing 6 M guanidinium hydrochloride and 1 mM TCEP. Purification of **precursor protein 1** was performed by Ni-NTA in buffer including 6 M guanidinium hydrochloride. The result of the purification was shown in **Figure 4-3**. The band corresponding to the molecular weight of **precursor protein 1** (63 kDa) was found in **lane 5-7** which were elutions collected by the addition of

imidazole. Although there still were impurities in the collected fraction, the author proceeded for further experiments.

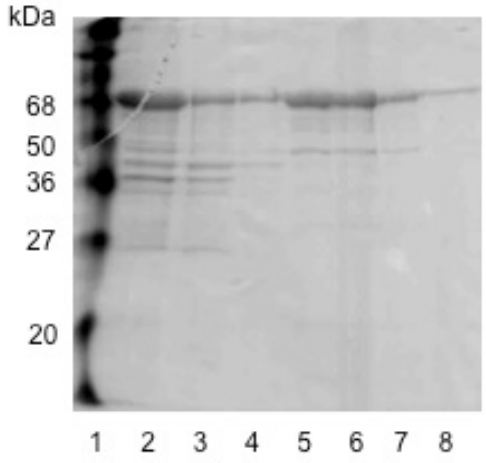

Figure 4-3. SDS-PAGE showing purification of **precursor protein 1** (MW= 63k Da) **Precursor protein 1** was purified by affinity chromatography using Ni-NTA. The collected cells were sonicated in buffer and centrifuged. The precipitation was dissolved with guanidinium hydrochloride (**lane 2**). The solution was loaded on to the Ni-NTA and then Ni-NTA was washed the buffer (**lane 3**: flow-through, **lane 4**: wash). The **precursor protein 1** bound to the column was eluted by the addition of imidazole (**lane 5-8**).

To obtain **fragment 2**, purified **precursor protein 1** was refolded by dialysis against 25 mM HEPES (pH7.5) including 150 mM NaCl and 10 % glycerol as described by Plotnikov and coworkers[3], with 50 mM MESNA. SDS-PAGE gel on **Figure 4-4** shows the result on refolding of the intein portion in **precursor protein 1**. **Lane 1** and **2** show contents in the solution before and after refolding, respectively. Refolding was performed against a buffer containing MESNA, which triggers thio-induced cleavage to liberate **fragment 2** from **precursor protein 1**. Bands corresponding to **fragment 2** (35 kDa) and tag including *Mxe gyrA* intein, CBD and His-tag (28 kDa) were found in **lane 2**. Result suggests that the thiol-induced cleavage was occurred as the intein portion in **precursor protein 1** folded in presence of MESNA to give **fragment 2**.

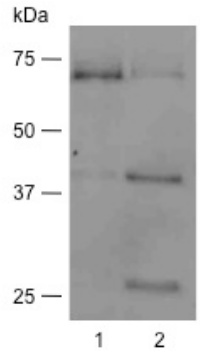

Figure 4-4. SDS-PAGE showing refolding of **precursor protein1** and release of **fragment 2**. **Precursor protein 1** dissolved in guanidinium hydrochloride (**lane 1**) was refolded by dialysis against 25 mM HEPES pH7.5, 150 mM NaCl, 10 % glycerol and 50 mM MESNA. As a result, bands from **fragment 2** (35 kDa) and the fragment of the intein sequence, CBD and His-tag (28 kDa) were observed (**lane 2**).

- Synthesis of C-terminal building block, peptide 3, in Fmoc chemistry

Synthesis of C-terminal building block, **peptide 3** was summarized in **Scheme 4-2**.

Fmoc - NH - SAL - PEG resin

1) Piperidine (20 %) / NMP
2) Fmoc-A.A.-OBt

H-Cys(Trt) - Leu - Ala - Gly - Asn(Trt) - Ser(*t*Bu) - Ile - Gly - Phe - Ser(*t*Bu) - His(Trt) - His(Trt) - Ser(*t*Bu) - Ala - Trp(Boc) - Leu - Vla - Val - Leu - Pro - Ala -Glu(O*t*Bu) - Glu(O*t*Bu) - Glu(O*t*Bu) - Leu - Val - Glu(O*t*Bu) - Ala - Asp(O*t*Bu) -Glu (O*t*Bu) - Ala - Gly- Ser(*t*Bu) - Val - Tyr(*t*Bu) - Ala - Gly - Ile - Leu - Ser(*t*Bu) -Tyr(*t*Bu) - Gly - Gly - Val - Gly - Phe - Phe - Leu - Phe - Ile - Leu - Val -Val - Ala - Ala - Val- Thr(*t*Bu) - Leu - Cys (Trt) - Arg(Pbf) - Leu - Arg(Pbf) - Ser(*t*Bu) - Pro - Pro - Lys(Boc) - Lys(Boc) - Gly - Leu - Gly - NH_2 - SAL - PEG resin

1) TFA, 1,2-Ethaneditiol, thioanisole
2) RP-HPLC

H-Cys - Leu - Ala - Gly - Asn - Ser - Ile - Gly - Phe - Ser - His - His - Ser - Ala - Trp -Leu - Vla - Val - Leu - Pro - Ala -Glu - Glu - Glu - Leu - Val - Glu - Ala - Asp -Glu - Ala -Gly- Ser - Val - Tyr - Ala - Gly - Ile - Leu - Ser -Tyr - Gly - Gly - Val - Gly - Phe - Phe - Leu - Phe - Ile - Leu - Val -Val - Ala - Ala - Val- Thr - Leu - Cys - Arg - Leu - Arg - Ser - Pro - Pro - Lys - Lys - Gly - Leu - Gly - NH_2

Scheme 4-2. Synthesis of **peptide 3**

Starting from NH_2-SAL-PEG resin, the C-terminal segment, FGFR3 EJM-TM-IJM (residues 339-407) was synthesized by Fmoc chemistry. The peptide component was cleaved from the resin by treatment with TFA. Purification using RP-HPLC was performed a linear gradient of formic acid/ water (3:2) and formic acid/ 1-propanol (4:1) at a flow rate of 1.75 ml/min. The RP-HPLC chromatogram was shown in **Figure 4-5**. The content of the main peak shown with an arrow on **Figure 4-5** was characterized with MALDI-TOF mass spectrometry. The mass number found agreed with the calculated value for the desired product (found m/z: 7247.6, calcd for $[M+H]^+$: 7245.4). The C-terminal building block, **peptide 3**, was obtained using peptide synthesis.

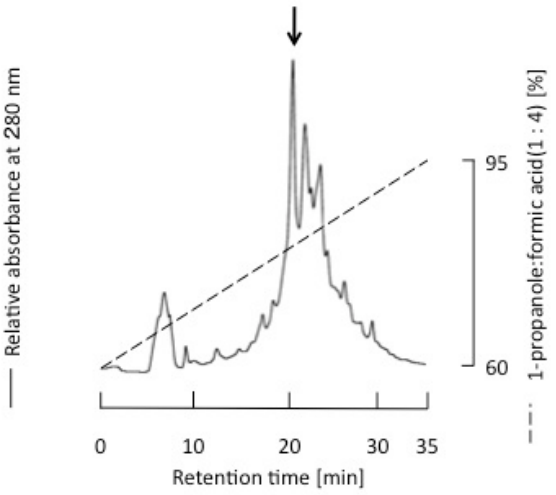

Figure 4-5. RP-HPLC elusion profiles of the purification of **peptide 3**. The details of conditions are indicated under the chromatogram.

- Native chemical ligation of fragment 2 at the C-terminus and peptide 3

Fragment 2 and **peptide 3** were mixed in 20 mM HEPES pH 7.5 containing 50 mM

MESNA, 30 mM OG, 3 mM TCEP and 500 mM NaCl at 4 °C or 37 °C overnight for the ligation. The reaction was monitored by SDS-PAGE. The result was shown in **Figure 4-6**. The band corresponding to ligation product (42 kDa) was found in the **lane 2** and **3**, which was shown with red arrow. In **Chapter 1**, it was described that the efficiency in the ligation reaction for the synthesis of the TM-IJM region sequence was higher when it was performed in presence of OG at a concentration below CMC. However, at the concentration below CMC, 15 mM, both building blocks were not soluble. Raising the OG concentration up to 30 mM allowed all of reactants to be soluble throughout the period of the reaction. It was also found, for this reaction, that the lower temperature at 4 °C kept the reactants soluble. At the higher temperature at 37 °C, some precipitates were observed during the reaction.

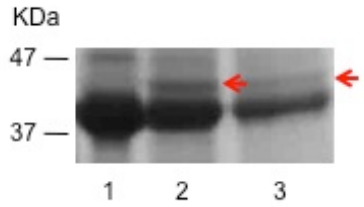

Figure 4-6. Ligation of FGFR3 ECD with thioester at the C-terminus (**lane 1**) and EJM-TM-IJM. The reaction was at 4 °C (**lane 2**) or 37 °C (**lane 3**) overnight. The molecular weight of ligation products, FGFR3 ECD-EJM-TM-IJM (23-407), was 42 kDa and the band from the ligation product was indicated the arrow in the SDS-PAGE gel.

Semi-synthesis of FGFR3 Y373C (23-422) using protein expression by mammalian cell

- Preparation of N-terminal building block, fragment 5, with expression by mammalian cells

For preparing the ECD of FGFR3, mammalian cells has a great advantage for its

production in a folded state. As it was observed that the production yield for the ECD with E. coli was not as high as expected, it was decided to examine the ECD preparation with mammalian cells. pFUSE ssIL2 FGFE3 Y373C ECD-Intein-PA tag vector was subcloned to express the precursor protein of FGFR3 Y373C ECD (23-372)-*Mxe gyrA* intein-PA tag (**precursor protein 4**), by HEK293S cells. The construct of the vector was shown in **Figure 4-7**.

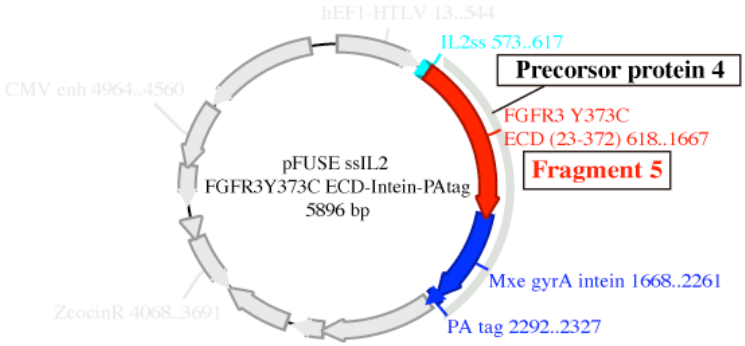

Figure 4-7. Construct of pFUSE ssIL2 FGFR3 Y373C ECD-Intein-PA tag vector

The vector was transfected to mammalian cells, HEK293S, to obtain the **precursor protein 4**. Purification of **precursor protein 4,** which was secreted from cells, was performed by NZ-1-Sepharose[4]. The result of purification for **precursor protein 4** was shown in **Figure 4-8 (A)**. The bands corresponding to **precursor protein 4** (62 kDa) with carbohydrate chains was found on the Western blot analysis. To purify **fragment 5**, the fragment was co-incubated with NZ-1-Sepharose in the solution of 25 mM HEPES pH 7.5 with 50 or 250 mM MESNA at 4 or 37 °C overnight. The result of the purification of **fragment 5** was shown in **Figure 4-8 (B)**. In the Western blot analysis, the single bands corresponding to **fragment 5** (38 kDa) with carbohydrate chains were found in **lane 2** and **4**. The bands corresponding to **precursor protein 4** and **fragment 5** were found in **lane 7-10**. **Fragment 5** was eluted from

NZ-1-Sepharose as the result of cleavage from **precursor protein 4** induced by MESNA at 4 °C overnight. **Fragment 5** was obtained relatively more effectively with the solution of 250 mM MESNA.

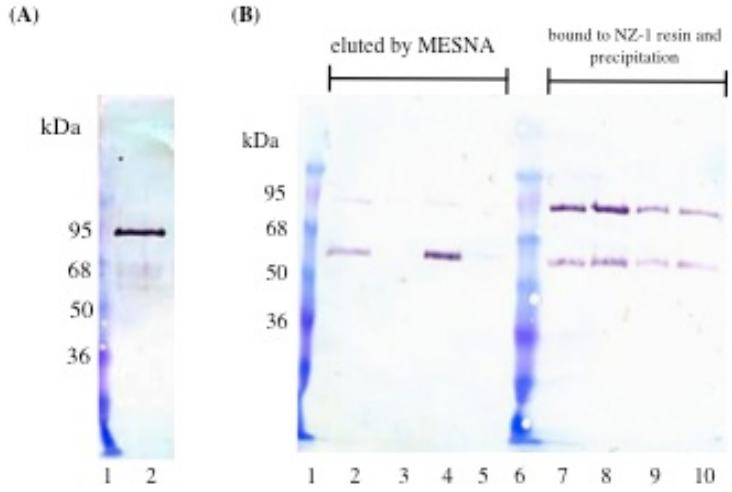

Figure 4-8. Western blot analysis of **precursor protein 4** and **fragment 5** using expression of mammalian cells, HEK293S. **(A)** SDS-PAGE was transferred to a membrane and the membrane was immunoblotted with FGFR-3 (H-100). **Precursor protein 4** was purified by NZ-1-Sepharose (**lane 2**). **(B)** SDS-PAGE was transferred to a membrane and the membrane was immunoblotted with FGFR-3 (H-100). **Fragment 5** was purified from NZ-1-Sepharose, which **precursor protein 4** bound, by incubation with solution of MESNA overnight (**lane 2**: 50 mM MESNA at 4 °C, **lane 3**: 50 mM MESNA at 37 °C, **lane 4**: 250 mM MESNA at 4 °C, **lane 5**: 250 mM MESNA at 37 °C). **Precursor protein 4**and **fragment 5** were also found from NZ-1-Sepharose and the precipitation (**lane 7**: rest of **lane 2**, **lane 8**: rest of **lane 3**, **lane 9**: rest of **lane 4**, **lane 10**: rest of **lane 5**).

- Synthesis of C-terminal building block, peptide 6, in Fmoc chemistry

Synthesis of C-terminal building block, **peptide 6** was summarized in **Scheme 4-3**.

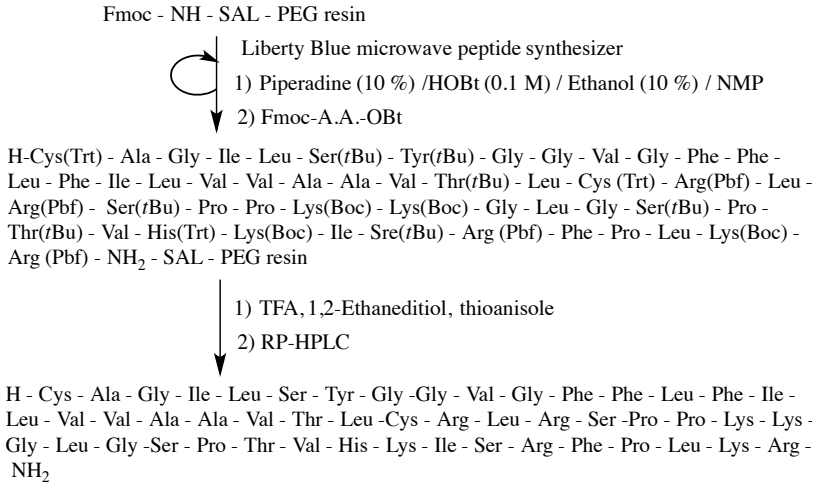

Scheme 4-3. Synthesis of **peptide 6**

Staring from NH_2-SAL-PEG resin, the C-terminal building block, FGFR3 Y373C EJM-TM-IJM (residues 373-422) was synthesized by Fmoc Chemistry using automated microwave peptide synthesizer, Blue Liberty (CEM corporation). The peptide component was cleaved from the resin by treatment with TFA. Purification was performed by RP-HPLC.

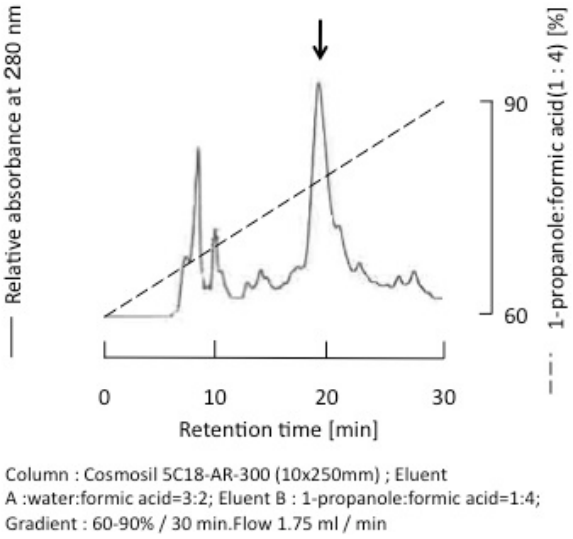

Figure 4-9. RP-HPLC elusion profiles of the purification of **peptide 6**. The details of conditions are indicated under the chromatogram.

Purification using RP-HPLC was performed a liner gradient of formic acid/ water (3:2) and formic acid/ 2-propanol (4:1) at a flow rate of 1.75 ml/ min. The RP-HPLC chromatogram was shown in **Figure 4-9**. The content of the main peak shown with an arrow on **Figure 4-9** was characterized with MALDI-TOF mass spectrometry. The mass number found agreed with the calculated value for the desired product (found m/z: 5320.0; calcd for $[M+H]^+$: 5314.9). The C-terminal building block, **peptide 6**, was obtained using peptide synthesis.

- Native chemical ligation of fragment 5 and peptide 6

Fragment 5 and **peptide 6** were mixed in 25 mM HEPES pH 7.5 containing 250 mM MESNA, 15 mM OG at 4 °C or 37 °C overnight for the ligation. The reaction was monitored by Western blot analysis. The result was shown in **Figure 4-10**. The band corresponding to the ligation product (43 kDa) with carbohydrate chains was found in the **lane 3**. The ligation product was found in the reaction at 4 °C. However, for the reaction at 37 °C, the ligation product and the building block were not found.

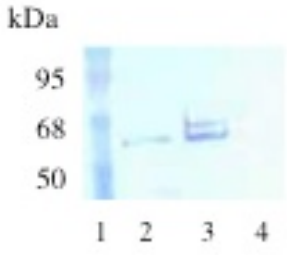

Figure 4-11. Western bolt analysis of ligation. SDS-PAGE was transferred to a membrane and the membrane was immunoblotted with FGFR-3 (H-100). **Fragment 5** was obtained (**lane 2**) and mixed with 1 mM **peptide 6** and 15 mM OG at 4 °C (**lane 3**) or 37 °C (**lane 4**) overnight.

Discussion

The semi-synthetic FGFR3 (23-407) was obtained using native chemical ligation of the ECD expressed by *E. coli*, and the chemically synthesized EJM-TM-IJM peptide. There were some problems in this strategy. The yield in this was too small to proceed for an analysis on the TM-JM region by spectroscopic experiments and the refolding of ECD was required after the ligation reaction. The expression of **precursor protein 1** by mammalian cells was introduced to solve the problem of the ECD refolding. However, the **precursor protein 1** was not obtained with the expression by mammalian cells. The reason seems to be the fact that the employed sequence, FGFR3 (23-338), lacks the C-terminal portion of the Ig domain. As we re-designed the ECD to the sequence of FGFR3 (23-372), which contains full sequence of the Ig domain, its expression by the mammalian cells was confirmed. Y373C mutation was introduced for a synthetic purpose, which provides Cys residues for ligation site. Y373C mutation is known as a pathogenic mutation for FGFR3 but it is also known that it still has ligand dependent kinase activity [5,6]. It is possible to analyze the structural change of TM-JM region upon ligand binding to semi-synthetic FGFR3 Y373C.

As it was shown in **Figure 4-11**, the semi-synthetic FGFR3 Y373C was observed. The yield for the ligation reaction was higher than that of FGFR3 (23-407) of which ECD was prepared by *E. coli*. Difference in yield of the ligation reaction for the two proteins may be caused by structure of ligation site and solubility of building block. The ECD building block prepared by the mammalian cells was soluble in the aqueous buffer with 15 mM OG of which concentration allow solubilizing the TM-JM sequence. However, this concentration did not give a clear solution for the reaction with the ECD building block prepared by *E. coli*. It was required to raise the OG concentration up to

30 mM OG, suggesting that the ECD building block prepared by *E. coli* aggregated in the buffer.

Although more effort is required to proceed to spectroscopic analysis on the receptor, results herein show proof-of-concept for the semi-synthesis of FGFR3.

Material and methods

pUC57 FGFR3 ECD encoding FGFR3 ECD (residues 1-410) and primers were synthesized by Hokkaido System Science Co., Ltd. (Hokkaido, Japan). DNA polymerase, KOD-Plus-Neo, and DNA ligase, Ligation high Ver.2, were purchased from TOYOBO (Osaka, Japan). pTXB1 vector encoding encoding *Mxe gyrA* intein and CBD and restriction enzyme, Nde1, Sap1, BamH1 an Xho1 were purchased from New England BioLab Inc. (New England, USA). *E. coli* DH5α, PrimeSTAR® Mutagenesis Basal Kit and In-Fusion® HD Cloning Kit were purchased from TaKaRa (Shiga, Japan). One Shot® BL21(DE3) pLysS Chemically Competent *E. coli* was purchased from Life Technology (Carlsbad, CA, USA). Ni-NTA was purchased from QIAGEN (Hilden, Germany). Pre-Stained Protein Markers (Broad range) was purchased from Nacalai Tesque (Kyoto, Japan). pBlue Script ll SK (+) FGFR3 (cDNA fragment) encoding human FGFR3 (residues 1-806) was purchased from Kazusa DNA Research Institute (Chiba, Japan). pFUSE IL2ss PA tag vector, NZ-1 resin and HEK293S cells were obtained from Prof. Junichi Takagi at Institute for Protein Research, Osaka university. For Western bolt analysis, antibody against FGFR3 (H-100; sc-9007) and Anti-rabbit HRP conjugated antibody (W4011) were purchased from Santa Cruz Biotechnology (CA, USA) and Promega (WI, USA), respectively. Fmoc-NH_2-SAL-PEG resin was purchased from WATANABE CHEM, IND., LTD.

(Hiroshima, Japan). Amino acid derivatives were purchased from the Peptide Institute Inc. (Osaka, Japan). The DNA sequencing process of obtained vector was entrusted to Hokkaido System Science Co., Ltd. (Hokkaido, Japan). For PCR, TaKaRa PCR Thermal Cycler Dice® (Shiga, Japan) was used. The peptide mass number was determined using a MALDI-TOF MS autoflex™ (Bruker, Germany). The matrix used was sinapinic acid and peptides were dissolved in a mixture of formic acid and trifluoroethanol.

Semi-synthesis of FGFR3 (residues 23-407) using the N-terminal building block using the expression of *E. coli*

- Expression of precursor protein 1 and purification of N-terminal building block, fragment 2

PCR products encoding FGFR3 ECD (residues 23-338) with Nde1 site at the 5' end and Sap1 site at the 3' end site were amplified from pUC57 FGFR3ECD vector encoding FGFR3 ECD (residues 1-410) by PCR using the following primers; left primer: 5'-GGTGGTCATATGGAATCCCTGGGTACCGAGC-3', right primer: 5'-GGTGGTTGCTCTTCCGCACGTGTATTCGCCAGCATC-3'. The amplified PCR products and pTXB1 vector encoding *Mxe gyrA* intein and CBD were cleaved by restriction enzyme, Nde1 and Sap1, and they were ligated to obtain pTXB1 FGFR3 ECD vector which was coded FGFR3ECD, intein and CBD. His tag was inserted to the C-terminus of CBD in pTXB1 FGFR3 ECD vector using PrimeSTAR® and the following primers; left primer: 5'-CAACACCATCATCATCATCATTGACTGCAG GAAGGGGAT-3', right primer: 5'-TCAATGATGATGATGATGGTGTTGAAGCTG CCACAAGGC-3'. The obtained pTXB1-His tag FGFR3ECD vector encoding

FGFR3 ECD (residues 22-407)-*Mxe gyrA* intein-CBD-His tag was transformed into *E. coli* BL21 (DE3) pLysS cells. The cells were precultured in LB medium (20 mL) at 37 °C overnight. Cells were cultured in LB medium (1 L) at 37 °C for 1-2 h, induced with 1 mM IPTG at 18 °C overnight and centrifuged. Cells were sonicated with 25 mM phosphate buffer (pH7.5) containing 150 mM NaCl, 2 mM EDTA and 10 % glycerol. Following centrifugation, the pellet including the recombinant protein was dissolved in 6 M guanidinium hydrochloride and 1 mM TCEP in 100 mM Tris-HCl (pH7.5) at 37 °C overnight. The solubilized recombinant protein was added to Ni-NTA resin. Ni-NTA resin, which the recombinant protein was bound, was washed with 25 mM imidazole and 6 M guanidinium hydrochloride in 100 mM Tris-HCl (pH7.5). The recombinant protein was eluted from Ni-NTA resin with 250 mM imidazole and 6 M guanidinium hydrochloride in 100 mM Tris-HCl (pH7.5). The purification was monitored by SDS-PAGE. The purified recombinant protein with guanidinium hydrochloride was refolded by dialysis against 25 mM HEPES buffer pH7.5 containing 150 mM NaCl, 10 % glycerol and 25 mM MESNA to obtain FGFR3 ECD (residues 22-338) with thioester at the C-terminus. The refolding was monitored by SDS-PAGE.

- Synthesis of C-terminal building block, peptide 3

Fmoc-NH_2-SAL-PEG resin (0.24 mmol/g, 1.04 g) was treated with 20 % piperidine/ NMP solution (1x 5 min, 1x 25 min), washed with NMP (6x 1 min). A solution of Fmoc-amino acid (1.0 mmol), HOBt (1.0 mmol), HBTU (0.9 mmol) and DIEA (2.0 mmol) in DMF was added to the resin and stirred for 30 min. After finishing the coupling, the resin was washed with NMP (6x 1min) and added the capping solution of

acetic anhydride (10 %) and DIEA (5 %) in NMP (1x 5 min). These procedures were repeated to obtain a protected peptide resin corresponding to the sequence of FGFR3 EJM-TM-IJM (residues 336-407); H-Cys(Trt)-Leu-Ala-Gly-Asn(Trt)-Ser(*t*Bu)-Ile-Gly-Phe-Ser(*t*Bu)-His(Trt)-His(Trt)-Ser(*t*Bu)-Ala-Trp(Boc)-Leu-Val-Val-Leu-Pro-Ala-Glu(O*t*Bu)-Glu(O*t*Bu)-Glu(O*t*Bu)-Leu-Val-Glu(O*t*Bu)-Ala-Asp-Glu(O*t*Bu)-Ala-Gly-Ser(*t*Bu)-Val-Tyr(*t*Bu)-Ala-Gly-Ile-Leu-Ser(*t*Bu)-Tyr(*t*Bu)-Gly-Gly-Val-Gly-Phe-Phe-Leu-Phe-Ile-Leu-Val-Val-Ala-Ala-Val-Thr(*t*Bu)-Leu-Cys(Trt)-Arg(Pbf)-Leu-Arg(Pbf)-Ser(*t*Bu)-Pro-Pro-Lys(Boc)-Lys(Boc)-Gly-Leu-Gly-NH_2-SAL-PEG resin. The protected peptide resin (250 mg) was treated with a mixture of TFA (4.125 ml), thioanisole (250 μl), phenol (250 mg), ethandithiol (125 μL) and water (250 μl) at room temperature for 2 h 30 min. After the deprotection, cold ether was added to the mixture and the resulting precipitate was wash with ether and then dissolved in TFA. The solution was passed through a filter and precipitated by the addition of cold ether. The precipitate was washed with ether, and mixed with aqueous acetonitrile and freeze-dried to give the crude powder. Purification was performed on a Cosmosil column (10x 250 mm, 5C18-AR-300, Nakalai Tesque), and a linear gradient of formic acid/ water (3:2) and formic acid/ 1-propanol (4:1) at a flow rate of 1.75 mL/ min. The crude powder was dissolved in 70 % TFA with water and injected into the column. Peaks were collected and freeze-dried. As a result, a desired peptide was obtained; H-Cys-Leu-Ala-Gly-Asn-Ser-Ile-Gly-Phe-Ser-His-His-Ser-Ala-Trp-Leu-Val-Val-Leu-Pro-Ala-Glu-Glu-Glu-Leu-Val-Glu-Ala-Asp-Glu-Ala-Gly-Ser-Val-Tyr-Ala-Gly-Ile-Leu-Ser-Tyr-Gly-Gly-Val-Gly-Phe-Phe-Leu-Phe-Ile-Leu-Val-Val-Ala-Ala-Val-Thr-Leu-Cys-Arg-Leu-Arg-Ser-Pro-Pro-Lys-Lys-Gly-Leu-Gly-NH_2 (3-5 mg, MAS (MALDI) found for m/z: 7247.6, calcd for [M+H]+: 7245.4).

- Native chemical ligation of fragment 2 and peptide 3

FGFR3 ECD (residues 22-338) with thioester at the C-terminus (1 mg/mL, 50 μL) and FGFR3 EJM-TM-IJM (residues 239-407) peptide with cysteine at the N-terminus (50 nmol) were dissolved in 20 mM HEPES buffer pH7.5 including MESNA (2.5 μmol), OG (1.5 μmol), NaCl (25 μmol) and TCEP (0.15 μmol). The solution was stirred at 4 °C or 37 °C overnight. The reaction was monitored by SDS-PAGE.

Semi-synthesis of FGFR3 Y373C (residues 23-422) using the N-terminal building block by expression of mammalian cell

-Expression precursor protein 4 by mammalian cells and preparation of fragment 5

PCR products encoding FGFR3 Y373C ECD (residues 23-372) with the insertion site of pFUSE ssIL2 PA tag vector at the 5' end and the fusion site of *Mxe gyrA* intein at the 3' end site were amplified from pBlue Script ll SK (+) FGFR3 (cDNA fragment) vector encoding human FGFR3 by PCR using the following primers; left primer: 5'-GCACTAAGTCTTGCAGAGTCCTTGGGGACGGAGCAG-3', right primer: 5'-CACACTGCCCGCCTCGTCAGCCTC-3'. PCR products encoding *Mxe gyrA* intein with the fusion site of *Mxe gyrA* intein site at the 5' end and the insertion site of pFUSE ssIL2 PA tag vector site at the 3' end site were amplified from pTXB1 vector by PCR using the following primers; left primer: 5'-GAGGCGGGCAGTGTGT GCATCACGGGAGATGCAC-3', right primer: 5'-TGGCATGGCAACGCCGAGGCC TGAGTTCAGACC-3'. The linearized vector of pFUSE ssIL2 PA tag was amplified from pFUSE ssIL2 PA tag by PCR using the flowing primer; left primer:

5’-GGCGTTGCCATGCCAGGTGCCG-3’, right primer: 5’-TGCAAGACTTAGT GCAATGCAAGACAGGAGTTGC-3’. The PCR products encoding FGFR3 Y373C ECD (residues 23-372) and *Mxe gyrA* intein and the The linearized vector of pFUSE ssIL2 PA tag were mixed with In-Fusion HD Enzyme Premix to obtain pFUSE ssIL2 FGFE3 Y373C ECD-Intein-PA tag vector encoding precursor protein 4. pFUSE ssIL2 FGFE3 Y373C ECD-Intein-PA tag vector transfected to HEK293S cells by transfection regent, X-tremeGENE HP DNA for 3 days. After the transfection, the medium of transfected cell was added to the NZ-1-Sepharose and incubated for 2 hours at 4 °C. The NZ-1-Sepharose with precursor protein 4 was washed by 25 mM HEPES pH 7.5 buffer containing 150 mM NaCl and the purification of precursor protein 4 was monitored by SDS-PAGE and Western blotting. 250 or 50 mM MESNA was added to the NZ-1-Sepharose, which precursor protein 4 binds, to obtain and purify fragment 5. The purification of fragment 5 was monitored by SDS-PAGE and Western blotting.

- Synthesis of peptide 6

Starting from Fmoc-NH_2-SAL-PEG resin (0.24 mmol/g, 1.04 g), peptide chain elongation was carried out using a automated microwave peptide synthesizer, Blue Liberty (CEM corporation). Protected peptide resin corresponding to the sequence of FGFR3 EJM-TM-IJM (residues 373-422) was obtained; H-Cys(Trt)-Ala-Gly-Ile-Leu-Ser(*t*Bu)-Tyr(*t*Bu)-Gly-Gly-Val-Gly-Phe-Phe-Leu-Phe-Ile-Leu-Val-Val-Ala-Ala-Val-Thr(*t*Bu)-Leu-Cys(Trt)-Arg(Pbf)-Leu-Arg(Pbf)-Ser(*t*Bu)-Pro-Pro-Lys(Boc)-Lys(Boc)-Gly-Leu-Gly-NH_2-SAL-PEG resin. The protected peptide resin (250 mg) was treated with a mixture of TFA (4.125 ml), thioanisole (250 μl), phenol (250 mg), ethandithiol (125 μL) and water (250 μl) at room temperature for 2 h 30 min. After the deprotection, cold ether was added to the mixture and the resulting precipitate was

wash with ether and then dissolved in TFA. The solution was passed through a filter and precipitated by the addition of cold ether. The precipitate was washed with ether, and mixed with aqueous acetonitrile and freeze-dried to give the crude powder. Purification was performed on a Cosmosil column (10x 250 mm, 5C18-AR-300, Nakalai Tesque), and a linear gradient of formic acid/ water (3:2) and formic acid/ 1-propanol (4:1) at a flow rate of 1.75 mL/ min. The crude powder was dissolved in 70 % TFA with water and injected into the column. Peaks were collected and freeze-dried. As a result, a desired peptide was obtained; H-Cys--Ala-Gly-Ile-Leu-Ser-Tyr-Gly-Gly-Val-Gly-Phe-Phe-Leu-Phe-Ile-Leu-Val-Val-Ala-Ala-Val-Thr-Leu-Cys-Arg-Leu-Arg-Ser-Pro-Pro-Lys-Lys-Gly-Leu-Gly-NH_2 (3-5 mg, MAS (MALDI) found m/z: 5320.0; calcd for $[M+H]^+$: 5314.9).

- Native chemical ligation of fragment 5 and peptide 6

FGFR3 Y373C ECD (residues 22-372) with thioester at the C-terminus (50 μL) and FGFR3 Y373C EJM-TM-IJM (residues 373-422) peptide with cysteine at the N-terminus (50 nmol) were dissolved in 25 mM HEPES buffer pH7.5 including MESNA (12.5 μmol) and OG (0.75 μmol). The solution was stirred at 4 °C or 37 °C overnight. The reaction was monitored by SDS-PAGE and Western blotting.

1. Severinov, K., and Muir, T. W. Expressed protein ligation, a novel method for studying protein-protein interactions in transcription, *J. Biol. Chem.* **273**, 16205-16209 (1998)
2. Muir, T. W., Sondhi, D., and Cole, P. A. Expressed protein ligation: a general method for protein engineering, *Proc. Natl. Acad. Sci. U. S. A.* **95**, 6705-6710 (1998)
3. Plotnikov, A. N., Hubbard, S. R., Schlessinger, J., and Mohammadi, M. Crystal structures of two FGF-FGFR complexes reveal the determinants of ligand-receptor specificity, *Cell* ***101***, 413-424 (2000)
4. Fujii, Y., Kaneko, M., Neyazaki, M., Nogi, T., Kato, Y., and Takagi, J. PA tag: a versatile protein tagging system using a super high affinity antibody against a dodecapeptide derived from human podoplanin, *Protein Expr. Purif.* **95,** 240-247 (2014)
5. Rousseau, F., el Ghouzzi, V., Delezoide, A. L., Legeai-Mallet, L., Le Merrer, M., Munnich, A., and Bonaventure, J. Missense FGFR3 mutations create cysteine residues in thanatophoric dwarfism type I (TD1), *Hum. Mol. Genet.* ***5***, 509-512 (1996)
6. Adar, R., Monsonego-Ornan, E., David, P., and Yayon, A. Differential activation of cysteine-substitution mutants of fibroblast growth factor receptor 3 is determined by cysteine localization, *J. Bone Miner. Res.* **17**, 860-868 (2002)

Summary

It has been over two decades since the ligand binding-induced dimerization triggering RTK activation model was first established[1]. This model has provided the basis for studies on the molecular mechanism of RTK activation. Recent findings, such as the existence of preformed dimers on the plasma membrane[2-4] or detailed analysis on the negative cooperativity [5] suggests this initial model needs to be reconsidered.

In the case of preformed dimers, the inhibitory effect must be overcome by a structural change in the receptor. McLaughlin et al. have suggested that, for EGFR, this inhibitory effect is regulated by the interaction between the intracellular juxtamembrane (IJM) region and the inner leaflet of the membrane, or more specifically PIP_2[6-8]. Pike et al. have suggested that the IJM region is involved in the regulation of negative cooperativity, which also implies that the extracellular and IJM regions are coupled to the mechanism regulating receptor function[5]. Now, it is clear that the dimerization is not enough for the activation, but there seems to be a sequential structural change in the dimer upon ligand binding from the outside to inside or even, more interestingly, from the inside to the outside (i.e. negative cooperativity).

Regarding FGFRs, there is one interesting report that suggests that FGFR2 exists as preformed dimers at the membrane[9]. Ladbury et al. found[9] that growth factor receptor-bound protein 2 (Grb2) binds to a proline-rich sequence at the C-terminus of FGFR2 prior to growth factor stimulation. They demonstrated that Grb2 binds to FGFR2 in a 2:2 stoichiometry and retains basal activity. Upon stimulation, Grb2 is dissociated from the receptor, which allows for full activation of downstream signaling.

They suggest that the Grb2 dimer stabilizes the FGFR2 preformed dimer. This model implies that a structural or change in orientation within the dimer upon binding to the ligand can be the key factor for activation.

To elucidate this possible mechanism, the transmembrane (TM) and the juxtamembrane (JM) regions, which are the missing link, must be analyzed. In addition, data demonstrating that mutations affecting receptor function are located in the TM region indicate that the TM and JM regions play an active role in the activation mechanism, and should stimulate further studies on the structure and chemistry of these regions. Results reported in this thesis contribute to the structural characterization of the region and offer a framework for future studies of the TM-IJM region to further our understanding of the FGFR activation mechanism. In this chapter, results shown in previous chapters are summarized and a model for an activation mechanism of FGFR3 is established. Furthermore, research prospects using semi-synthetic receptors are discussed.

- Model for the activation mechanism of FGFR3

The mechanism that emerges from structural and biochemical studies is one in which the FGF ligand binds to the extracellular domain (ECD) of the receptor in a 1:1 complex. This complex is thought to form a symmetric dimer in the activated state[10]. The ligand binds to two of the immunoglobulin-like extracellular subdomains, D2 and D3. These two subdomains and the D2-D3 linker are necessary and sufficient for ligand binding. The D1 subdomain, together with the D1-D2 linker, play an autoregulatory role for the

receptor function[10]. High resolution structures of the activated kinase domains of FGFR1-3 reveal them to be asymmetric dimers[11,12]. Importantly, Schlessinger and coworkers demonstrated that formation of the asymmetric dimer between the activated FGFR1 kinase domains is required for transphosphorylation of FGFR in FGF-stimulated cells[11].

The major question addressed in this thesis is how the proposed structural changes in the extracellular and intracellular regions are coupled. For the purpose of this study, the premise that preformed dimers exist at the membrane is used. Several lines of evidence, especially the rigorous studies performed by Hristova et al.[13-15], suggest that the TM regions from FGFR3 dimerize in the lipid bilayer. In **Chapter 3**, the differences in the TM helices dimer interface of wild type and constitutively active mutants is examined. The working theory is that when the receptor is in the inactive state, prior to ligand binding, the dimer interface in the TM helices is observed for the wild type sequence. As shown in **Figure 5-1**, the association between S378-G382 in the TM helices contributes to inactive dimer structure formation. The S378-G382 sequence can be classified as a GxxxG-like motif that facilitates association of TM helices.

Another structural observation suggesting that the wild type structure represents the inactive state is that the wild type IJM region is bound to the acidic membrane. The basic IJM region in the inactive state can bind to the acidic inner leaflet of the plasma membrane. In addition, it is possible that the IJM region interacts with PIP_2, which can drive the association of the regions themselves. By associating with the membrane, the IJM regions can maintain the rest of the intracellular region in an inactive orientation.

The precise structure or arrangement relative to the membrane of the inactive FGFR3 intracellular region is unknown. However, based on the activation model of EGFR it can be hypothesized that the binding of the IJM region to the membrane results in an inhibitory effect, which prevents the kinase regions from interacting for transphosphorylation[16-18].

Moreover, it can be assumed that sequences containing the G380R or A391E constitutively active mutations represent the structure of this region in the active state. As mentioned in **Chapter 3**, the results of solid-state NMR experiments suggest that introduction of these mutations induces a change in the dimer interface of the TM helices. To date, the TM helices association site has not been identified in either of the sequences. However, the results of polarized Fourier transform infrared spectroscopy (FT-IR) experiments indicate that the structural rearrangement of TM helices containing the mutation affects the relative orientation of the TM helices, observed as a change in the TM helix tilt relative to the membrane. One of the important outcomes of this study is the demonstration that when the TM helix is "standing up" relative to the membrane, the IJM region is released from the membrane. This suggests a hypothesis specifying that in the intact system, when ligands bind to the extracellular regions, a structural rearrangement of the TM helices dimer occurs and, simultaneously, these helices "stand up" in the membrane, which causes the release of the IJM regions from the membrane. The release of the IJM region allows the intracellular regions to orient for transphosphorylation.

The model described here resembles that one proposed for EGFR[16-18]. It should be

emphasized that the release of the IJM region from the inner leaflet of the plasma membrane as a result of active structure formation in the TM region, could be a common structural change in RTKs for the initiation of events inside the membrane. The results and structural model described in this thesis regarding the dimer structure of the TM helices differ from the high-resolution structure obtained by Bocharov et al. with solution NMR[19]. In their structure, the S378-G382 sequence is located at the opposite side of the dimer interface. Dimerization is mediated by the $YA^{374}X_2L^{377}X_2G^{380}X_2FF^{384}X_2IL^{388}X_2A^{391}X_2TL^{395}$ sequence. They propose that the dimer interface mediated by the S378-G382 sequence may be the one that leads to receptor activation. The difference in the obtained structures is due to the membrane mimicking system that each group employed. All structural analysis of the TM-IJM peptide in this thesis was performed in lipid bilayers. In contrast, Bocharov et al. performed the analysis of the TM region in a micelle environment. In a reconstituting system with micelles, restrictions such as membrane thickness do not exist. As previously mentioned, membrane thickness has an effect on TM helix orientation, which induces IJM dissociation from the membrane. Although the dimer interface is currently unknown, it can be hypothesized that the TM helices dimer structure in thicker membranes is similar to that obtained in micelles. Detailed structural analyses are required to further elucidate the TM-IJM region and the release of the IJM region from the membrane.

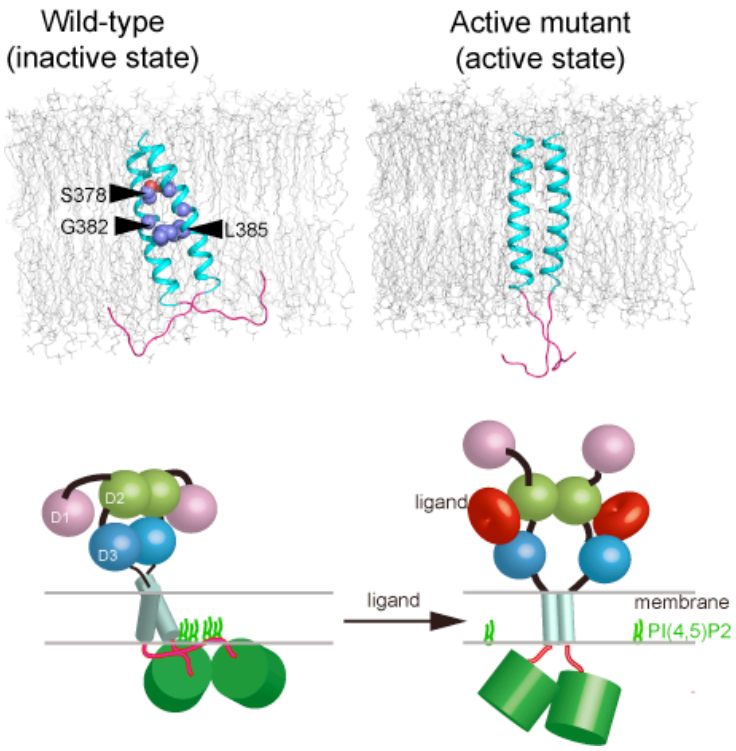

Figure 5-1. The FGFR3 activation model proposed in this study. The upper panel demonstrates the possible structure of the TM-IJM region in the inactive and active state. The lower panel describes the overall structural changes to FGFR3.

- Reseearch Prospective

The molecular characterization of the TM-IJM region performed in this study offers a framework for elucidating ligand binding-induced structural changes in this region; future studies will focus on capturing ligand induced changes in the TM helices dimer interface and the interaction between the IJM region and the membrane. Experimentally, studies such as these are difficult to carry out; therefore, reconstituting systems or artificial systems using semi-synthetic receptor are ideal for this purpose. As mentioned, semi-synthesis is accomplished by condensing chemically synthesized and expressed protein building blocks using ligation chemistry. A variety of specific labels and

modifications can be introduced into the chemically synthesized building blocks. Semi-synthesis of FGFR3 with stable isotope labels in the TM-IJM region is underway for use in structural analysis using solid-state NMR. Furthermore, this reconstituting system also provides an advantage in designing membrane systems with various lipid molecules. This research sheds light on the importance of lipid composition for membrane protein structure. Bio-membranes are a heterogeneous environment; and each type of lipid molecule has an effect on the biology on the membrane. The use of semi-synthetic receptors provides a new methodology for elucidating molecular mechanisms of biological phenomena occurring at the membrane.

Another advantage of semi-synthesis is that it provides a means to produce artificial receptors in the field of biomaterials. For example, in the case of RTK, if it were possible to design the extracellular region as an artificial protein fragment, we could also design a ligand molecule to regulate the signaling (**Figure 5-2**). One crucial and challenging technology in the field of regenerative medicine is the regulation cell growth. Synthesis of artificial receptors may contribute to the development of such biomaterials.

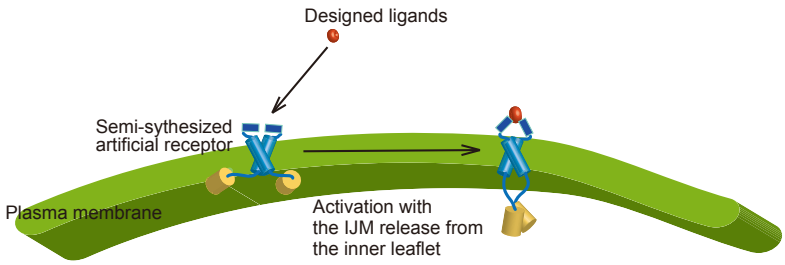

Figure 5-2. A concept of an artificial receptor as a biomaterial

1. Schlessinger, J. Signal transduction by allosteric receptor oligomerization. *Trends Biochem. Sci.* **13**, 443-7 (1988).
2. Chung, I. et al. Spatial control of EGF receptor activation by reversible dimerization on living cells. *Nature* **464**, 783-U163 (2010).
3. Moriki, T., Maruyama, H. & Maruyama, I.N. Activation of preformed EGF receptor dimers by ligand-induced rotation of the transmembrane domain. *J. Mol. Biol.* **311**, 1011-1026 (2001).
4. Sako, Y., Minoghchi, S. & Yanagida, T. Single-molecule imaging of EGFR signalling on the surface of living cells. *Nat. Cell Biol.* **2**, 168-72 (2000).
5. Adak, S., Yang, K.S., Macdonald-Obermann, J. & Pike, L.J. The Membrane-proximal Intracellular Domain of the Epidermal Growth Factor Receptor Underlies Negative Cooperativity in Ligand Binding. *J. Biol. Chem.* **286**, 45146-45155 (2011).
6. McLaughlin, S., Smith, S.O., Hayman, M.J. & Murray, D. An electrostatic engine model for autoinhibition and activation of the epidermal growth factor receptor (EGFR/ErbB) family. *J. Gen. Phys.* **126**, 41-53 (2005).
7. McLaughlin, S. & Murray, D. Plasma membrane phosphoinositide organization by protein electrostatics. *Nature* **438**, 605-11 (2005).
8. Sato, T., Pallavi, P., Golebiewska, U., McLaughlin, S. & Smith, S.O. Structure of the membrane reconstituted transmembrane-juxtamembrane peptide EGFR(622-660) and its interaction with Ca2+/calmodulin. *Biochemistry* **45**, 12704-12714 (2006).
9. Lin, C.C., Meilo, F. A., Ghosh, R., Suen, K. M., Stagg, L. J., Kirkpatrick, J., Arold, S. T., Ahmed, Z. & Ladbury, J. E. Inhibition of Basal FGF Receptor Signaling by Dimeric Grb2. *Cell* **149**, 1514-1524 (2012).
10. Mohammadi, M., Olsen, S.K. & Ibrahimi, O.A. Structural basis for fibroblast growth factor receptor activation. *Cytokine Growth Factor Rev.* **16**, 107-137 (2005).
11. Bae, J.H., Boggon, T. J., Tomé, F., Mandiyan, V., Lax, I. & Schlessinger, J. Asymmetric receptor contact is required for tyrosine autophosphorylation of fibroblast growth factor receptor in living cells. *Proc. Natl. Acad. Sci. U. S. A.* **107**, 2866-2871 (2010).
12. Chen, H.B., Xu, C. F., Ma, J., Eliseenkova, A. V., Li, W., Pollock, P. M.,

Pitteloud, N., Miller, W. T., Neubert, T. A. & Mohammadi, M. A crystallographic snapshot of tyrosine trans-phosphorylation in action. *Proc. Natl. Acad. Sci. U. S. A.* **105**, 19660-19665 (2008).

13. Li, E., You, M. & Hristova, K. Sodium dodecyl sulfate - Polyacrylamide gel electrophoresis and Forster resonance energy transfer suggest weak interactions between fibroblast growth factor receptor 3 (FGFR3) transmembrane domains in the absence of extracellular domains and ligands. *Biochemistry* **44**, 352-360 (2005).
14. Li, E., You, M. & Hristova, K. FGFR3 dimer stabilization due to a single amino acid pathogenic mutation. *J. Mol. Biol.* **356**, 600-612 (2006).
15. You, M., Li, E. & Hristova, K. The achondroplasia mutation does not alter the dimerization energetics of the fibroblast growth factor receptor 3 transmembrane domain. *Biochemistry* **45**, 5551-5556 (2006).
16. Matsushita, C., Tamagaki, H., Miyazawa, Y., Aimoto, S., Smith, S. O. & Sato, T. Transmembrane helix orientation influences membrane binding of the intracellular juxtamembrane domain in Neu receptor peptides. *Proc. Natl. Acad. Sci. U. S. A.* **110**, 1646-1651 (2013).
17. Arkhipov, A., Shan, Y., Das, R., Endres, N. F., Eastwood, M. P., Wemmer, D. E., Kuriyan, J. & Shaw, D. E. Architecture and Membrane Interactions of the EGF Receptor. *Cell* **152**, 557-569 (2013).
18. Endres, N.F., Das, R., Smith, A. W., Arkhipov, A., Kovacs, E., Huang, Y., Pelton, J. G., Shan, Y., Shaw, D. E., Wemmer, D. E., Groves, J. T. & Kuriyan, J. Conformational Coupling across the Plasma Membrane in Activation of the EGF Receptor. *Cell* **152**, 543-556 (2013).
19. Bocharov, E.V., Lesovoy, D. M., Goncharuk, S. A., Goncharuk, M. V., Hristova, K. & Arseniev, A. S. Structure of FGFR3 Transmembrane Domain Dimer: Implications for Signaling and Human Pathologies. *Structure* **21**, 2087-2093 (2013).

Publications

Original papers

1. Tamagaki, H., Furukawa, Y., Yamagushi, R., Hojo, H., Aimoto, S. & Sato, T. Coupling of Transmembrane Helix Orientation To Membrane Release of the Juxtamembrane Region in FGFR3. *Biochemistry* **53**, 5000-5007 (2014)
2. Matsushita, C., Tamagaki, H., Miyazawa, Y., Aimoto, S., Smith, S. O. & Sato, T. Transmembrane helix orientation influences membrane binding of the intracellular juxtamembrane domain in *Neu* receptor peptides. *Proc. Natl. Acad. Sci. U. S. A.* **110**, 1646-1651 (2013)

Proceedings

1. Tamagaki, H., Yamaguchi, R. & Sato, T. Structural Characterization of the Transmembrane-Intracellular Juxtamembrane Region of FGFR3 and its Implication in the Activation Mechanism. *Peptide Science 2013*, 59-60 (2014)
2. Tamagaki, H., Aimoto, S. & Sato, T. Structure of the Transmembrane and the Intracellular Juxtamembrane of FGFR3 in Lipid Bilayers. *Peptide Science 2012*, 325-326 (2013)
3. Matsushita, C., Tamagaki, H., Aimoto, S., Smith, S. O. & Sato, T. Interaction of the Intracellular Juxtamembrane Region with Lipid Bilayers Depends on Relative Orientation of Transmembrane Regions in Dimer of Receptor Tyrosine Kinase. *Peptide Science 2012*, 327-328 (2013)
4. Matsushita, C., Miyazawa, Y., Tamagaki, H., Aimoto, S., Smith, S. O. & Sato,

T. Structural Difference between the Wild Type and the Constutively Active Mutant Transmembrane-Juxtamembrane Region of Receptor Tyrosine Kinase Revealed by Solid State NMR and Fluorescence Spectroscopy. *Peptide Science 2011*, 221-222 (2012)

5. Tamagaki, H., Furukawa, Y., Matsushita, C., Smith, S. O., Aimoto, S. & Sato, T. Studies on the Effect of Pathogenic Mutation in the Transmembrane Region Structure of FGFR3. *Peptide Science 2009*, 389-390 (2010)

6. Matsushita, C., Miyazawa, Y., Tamagaki, H., Aimoto, S., Smith, S. O. & Sato, T. Effect of a Constitutively Active Mutation in the Transmembrane Region on its Structure of the Juxtamembrane Region of the ErbB Receptor. *Peptide Science 2009*, 387-388 (2010)

Acknowledgment

This research presented in this thesis has been carried out at Institute for Protein Research (IPR), Osaka University.

The author wishes to express their special gratitude to Associate Professor Takeshi Sato and Professor Saburo Aimoto providing the environment and opportunities that have stimulated them to grow intellectually so many ways, as well as for kind guidance and helpful suggestion. This author is also deeply grateful to Dr. Hironobu Hojo, Dr. Toru Kawakami, Dr. Terukazu Nogi, Dr. Junichi Takagi, Dr. Hisashi Yagi and Dr. Yuya Asahina for their helpful discussions.

Furthermore, the author whishes to thank all of the members in Laboratory of Protein Organic Chemistry, Institute for Protein Research and special thanks are given to Ms. Junko Toga, Ms. Emiko Mihara, Ms. Ritsuko Yamaguchi and Ms. Natsuha Yoshida.

The author wishes to thank all of her family members for their encouragement and patience.

Finally, a research fellow of the Japan Society of the Promotion of Science and the Platform for Drug Discovery, Informatics, and Structural Life Science (a project funded through the Japanese Ministry of Education, Culture, Sports and Technology) are gratefully acknowledged.

February 2015

Hiroko Tamagaki